

**Weak lensing of the CMB: A harmonic approach**

Wayne Hu

*Institute for Advanced Study, Princeton, New Jersey 08540*

(Received 19 January 2000; published 25 July 2000)

Weak lensing of CMB anisotropies and polarization for the power spectra and higher order statistics can be handled directly in harmonic-space without recourse to real-space correlation functions. For the power spectra, this approach not only simplifies the calculations but is also readily generalized from the usual flat-sky approximation to the exact all-sky form by replacing Fourier harmonics with spherical harmonics. Counterintuitively, because of the nonlinear nature of the effect, errors in the flat-sky approximation do not improve on smaller scales. They remain at the 10% level through the acoustic regime and are sufficiently large to merit adoption of the all-sky formalism. For the bispectra, a cosmic variance limited detection of the correlation with secondary anisotropies has an order of magnitude greater signal-to-noise for combinations involving magnetic parity polarization than those involving the temperature alone. Detection of these bispectra will, however, be severely noise and foreground limited even with the Planck satellite, leaving room for improvement with higher sensitivity experiments. We also provide a general study of the correspondence between flat and all sky potentials, deflection angles, convergence and shear for the power spectra and bispectra.

PACS number(s): 98.70.Vc, 95.75.Pq, 98.80.Hw

**I. INTRODUCTION**

As the cosmic microwave background (CMB) photons propagate from the last scattering surface through intervening large-scale structure, they are gravitationally lensed. Weak lensing effects on the the temperature and polarization distributions of the cosmic microwave background are already a well-studied field. As in other aspects of the field, early work treating the effects on the temperature correlation function [1] has largely been superceded by harmonic space power spectrum analyses in the post Cosmic Background Explorer (COBE) era [2,3]. In harmonic space, the physical processes of anisotropy formation are most directly manifest. However for weak lensing in the CMB, correlation function underpinnings have typically remained, forcing transformations between real and Fourier space to define the effect in a small-angle (flat-sky) approximation. Exceptions include recent work on the non-Gaussianity of the lensed temperature field where a direct harmonic space approach has been taken [4,5].

In this paper, we provide a complete framework for the study of lensing effects in the temperature and polarization fields directly in harmonic space. Not only does this greatly simplify the power spectrum calculations but it also establishes a clear link between weak lensing power spectrum observables in wide-field galaxy surveys and CMB observables for cross-correlation studies. Furthermore, this approach is easily generalized to lensing on the full sky by replacing Fourier harmonics with spherical harmonics.

We show that, counterintuitively, corrections from employing an exact all-sky treatment are not confined to large angles. The second order nature of the effect brings in large scale power through mode coupling. Since the all-sky expressions are as simple to evaluate as their flat-sky approximations, which themselves are much simpler to evaluate than the correlation function analogues, they should be employed where full accuracy is required, e.g., for the analysis of precise measurements from CMB satellite missions.

Beyond the power spectrum, lensing induces three point correlations in the CMB through its correlation with secondary anisotropies [4,5], even when the intrinsic distribution at last scattering is Gaussian. Detection of these effects in the temperature maps, however, is severely limited by cosmic variance. The primary anisotropies themselves act at Gaussian noise for these purposes. In this case, the low level at which the CMB is polarized can be an asset not a liability. Three point correlations involving the polarization, where orientation plays a role, are most simply considered with their harmonic space analogue, the bispectrum. We introduce polarization and polarization-temperature bispectra and show that they can have signal-to-noise advantages over those involving the temperature alone.

The outline of the paper is as follows. In Sec. II, we treat the basic elements of the cosmological framework, CMB temperature and polarization, and weak lensing needed to understand these effects. Detailed derivations are presented in a series of Appendixes: Appendix A covers the all-sky weak lensing approach, Appendix B the evaluation of the all-sky formulas, and Appendix C the correspondence between the flat and all sky approaches for scalar, vector and tensor fields on the sky. The lensing effects on the power spectrum are treated in the flat-sky approximation in Sec. III and in the exact all-sky approach in Sec. IV. In Sec. V, we study the effects of lensing on the bispectra of the temperature and polarization distributions. We conclude in Sec. VI.

**II. FORMALISM**

In this section, we review and develop the formalism necessary for calculating lensing effects in the CMB. We review the relevant properties of the adiabatic cold dark matter (CDM) model in Sec. II A. In Sec. II B, we discuss the power spectra and bispectra of the temperature fluctuations, polarization and temperature-polarization cross correlation. Finally in Sec. II C, we review the properties of weak lensing relevant for the CMB calculation.

### A. Cosmological model

We work in the context of the adiabatic CDM family of models, where structure forms through the gravitational instability of the CDM in a background Friedmann-Robertson-Walker metric. In units of the critical density  $3H_0^2/8\pi G$ , where  $H_0 = 100h \text{ km s}^{-1} \text{ Mpc}^{-1}$  is the Hubble parameter today, the contribution of each component is denoted  $\Omega_i$ ,  $i = c$  for the CDM,  $b$  for the baryons,  $\Lambda$  for the cosmological constant. It is convenient to define the auxiliary quantities  $\Omega_m = \Omega_c + \Omega_b$  and  $\Omega_K = 1 - \sum_i \Omega_i$ , which represent the matter density and the contribution of spatial curvature to the expansion rate respectively. The expansion rate

$$H^2 = H_0^2 [\Omega_m (1+z)^3 + \Omega_K (1+z)^2 + \Omega_\Lambda] \quad (1)$$

then determines the comoving conformal distance to redshift  $z$ ,

$$D(z) = \int_0^z \frac{H_0}{H(z')} dz', \quad (2)$$

in units of the Hubble distance today  $H_0^{-1} = 2997.9h^{-1} \text{ Mpc}$ . The comoving angular diameter distance

$$D_A = \Omega_K^{-1/2} \sinh(\Omega_K^{1/2} D), \quad (3)$$

plays an important role in lensing. Note that as  $\Omega_K \rightarrow 0$ ,  $D_A \rightarrow D$ .

The adiabatic CDM model possesses a power spectrum of fluctuations in the gravitational potential  $\Phi$

$$\Delta_\Phi^2(k, z) = \frac{k^3}{2\pi^2} P_\Phi = A(z) \left( \frac{k}{H_0} \right)^{n-1} T^2(k), \quad (4)$$

where the transfer function is normalized to  $T(0) = 1$ . We employ the CMBFAST code [6] to determine  $T(k)$  at intermediate scales and extend it to small scales using analytic fits [7].

The cosmological Poisson equation relates the power spectra of the potential and density perturbations  $\delta$

$$\Delta_\Phi^2 = \frac{9}{4} \left( \frac{H_0}{k} \right)^4 \left( 1 + 3 \frac{H_0^2}{k^2} \Omega_K \right)^{-2} \Omega_m^2 (1+z)^2 \Delta_\delta^2, \quad (5)$$

and gives the relationship between their relative normalization

$$A(z) = \frac{9}{4} \left( 1 + 3 \frac{H_0^2}{k^2} \Omega_K \right)^{-2} \Omega_m^2 F(z) \delta_H^2. \quad (6)$$

Here  $\delta_H$  is the amplitude of present-day density fluctuations at the Hubble scale; we adopt the COBE normalization for  $\delta_H$  [8].  $F(z)/(1+z)$  is the growth rate of linear density perturbations  $\delta(z) = F(z) \delta(0)/(1+z)$  [9]

$$F(z) \propto (1+z) \frac{H(z)}{H_0} \int_z^\infty dz' (1+z') \left( \frac{H_0}{H(z')} \right)^3. \quad (7)$$

For the matter dominated regime where  $H \propto (1+z)^{3/2}$ ,  $F$  is independent of redshift.

Although we maintain generality in all derivations, we illustrate our results with a  $\Lambda$ CDM model. The parameters for this model are  $\Omega_c = 0.30$ ,  $\Omega_b = 0.05$ ,  $\Omega_\Lambda = 0.65$ ,  $h = 0.65$ ,  $Y_p = 0.24$ ,  $n = 1$ , and  $\delta_H = 4.2 \times 10^{-5}$ . This model has mass fluctuations on the  $8h \text{ Mpc}^{-1}$  scale in accord with the abundance of galaxy clusters  $\sigma_8 = 0.86$ . A reasonable value here is important since the lensing calculation is second order.

### B. CMB

We decompose the CMB temperature perturbation on the sky  $\Theta(\hat{\mathbf{n}}) = \Delta T(\hat{\mathbf{n}})/T$  into its multipole moments

$$\Theta(\hat{\mathbf{n}}) = \sum_{lm} \Theta_{lm} Y_l^m(\hat{\mathbf{n}}). \quad (8)$$

The polarization on the sky is represented by the trace-free symmetric Stokes matrix on the sky

$$\mathbf{P}(\hat{\mathbf{n}}) = {}_+X(\hat{\mathbf{n}})(\mathbf{m}_+ \otimes \mathbf{m}_+) - {}_-X(\hat{\mathbf{n}})(\mathbf{m}_- \otimes \mathbf{m}_-), \quad (9)$$

where

$${}_\pm X(\hat{\mathbf{n}}) = Q(\hat{\mathbf{n}}) \pm iU(\hat{\mathbf{n}}),$$

$$\mathbf{m}_\pm = \frac{1}{\sqrt{2}} (\hat{\mathbf{e}}_{\theta^\mp} \mp i \hat{\mathbf{e}}_\phi). \quad (10)$$

The complex Stokes parameter  ${}_\pm X$  is a spin-2 object which can be decomposed in the spin-spherical harmonics [11]

$${}_\pm X(\hat{\mathbf{n}}) = \sum_{lm} {}_\pm X_{lm\pm 2} Y_l^m(\hat{\mathbf{n}}). \quad (11)$$

We have assumed that the Stokes  $V$  parameter vanishes as appropriate for cosmological perturbations; for a full set add the term  $V \epsilon_{ij}$  to the polarization matrix, where  $\epsilon_{ij}$  is the Levi-Civita tensor.

Due to the parity properties of the spin-spherical harmonics

$${}_s Y_l^m \rightarrow (-1)^l {}_{-s} Y_l^m, \quad (12)$$

one introduces the parity eigenstates [12,13]

$${}_\pm X_{lm} = E_{lm} \pm iB_{lm}, \quad (13)$$

such that  $E_{lm}$  just like  $\Theta_{lm}$  has parity  $(-1)^l$  (“electric” parity) whereas  $B_{lm}$  has parity  $(-1)^{l+1}$  (“magnetic” parity). Density (scalar) fluctuations in linear theory only stimulate the  $E$  component of polarization.

The power spectra and cross correlation of these quantities is defined as

$$\langle X_{lm}^* X_{l'm'} \rangle = \delta_{l,l'} \delta_{m,m'} C_l^{XX'}, \quad (14)$$

where  $X$  and  $X'$  can take on the values  $\Theta$ ,  $E$ ,  $B$ . Note that the cross power spectra between  $B$  and  $\Theta$  or  $E$  have odd total parity and thus vanish assuming anisotropy formation is a parity invariant process.

The bispectrum is defined as

$$\langle X_{lm} X'_{l'm'} X''_{l''m''} \rangle = \begin{pmatrix} l & l' & l'' \\ m & m' & m'' \end{pmatrix} B_{ll'l''}^{XX'X''}, \quad (15)$$

and vanishes if the fluctuations are Gaussian. Even in the presence of non-Gaussianity due to nonlinear but parity-conserving sources, bispectra involving an even number of magnetic parity terms (including zero) vanish for  $l+l'+l'' = \text{odd}$  and those involving an odd number vanish for  $l+l'+l'' = \text{even}$ .

For a small section of the sky or high multipole moments, it is sufficient to treat the sky as flat. In the flat-sky approximation, the Fourier moments of the temperature fluctuations are given as

$$\Theta(\hat{\mathbf{n}}) = \int \frac{d^2\mathbf{l}}{(2\pi)^2} \Theta(\mathbf{l}) e^{i\mathbf{l}\cdot\hat{\mathbf{n}}}, \quad (16)$$

and the polarization as

$$\pm X(\hat{\mathbf{n}}) = - \int \frac{d^2\mathbf{l}}{(2\pi)^2} \pm X(\mathbf{l}) e^{\pm 2i(\varphi_l - \varphi)} e^{i\mathbf{l}\cdot\hat{\mathbf{n}}}, \quad (17)$$

where  $\varphi_l$  is azimuthal angle of  $\mathbf{l}$ . Again one separates the Stokes moments as

$$\pm X(\mathbf{l}) = E(\mathbf{l}) \pm iB(\mathbf{l}). \quad (18)$$

As in the all-sky case, the power spectra and cross correlations can be defined as with power spectra

$$\langle X^*(\mathbf{l}) X'(\mathbf{l}') \rangle = (2\pi)^2 \delta(\mathbf{l} - \mathbf{l}') C_{(l)}^{XX'}, \quad (19)$$

$$\langle X^*(\mathbf{l}) X'(\mathbf{l}') X''(\mathbf{l}'') \rangle = (2\pi)^2 \delta(\mathbf{l} - \mathbf{l}' - \mathbf{l}'') B_{(l,l',l'')}^{XX'X''}.$$

The power spectra for the fiducial CDM model with a cosmological constant ( $\Lambda$ CDM) model are shown in Figs. 1 and 2.

In Appendix C, we establish the correspondence between the all-sky and flat-sky spectra. For the power spectra and bispectra

$$C_l^{XX'} \approx C_{(l)}^{XX'},$$

$$B_{ll'l''}^{XX'X''} \approx \begin{pmatrix} l & l' & l'' \\ 0 & 0 & 0 \end{pmatrix} \times \sqrt{\frac{(2l+1)(2l'+1)(2l''+1)}{4\pi}} B_{(l,l',l'')}^{XX'X''}, \quad (20)$$

for sufficiently high  $l$ 's.

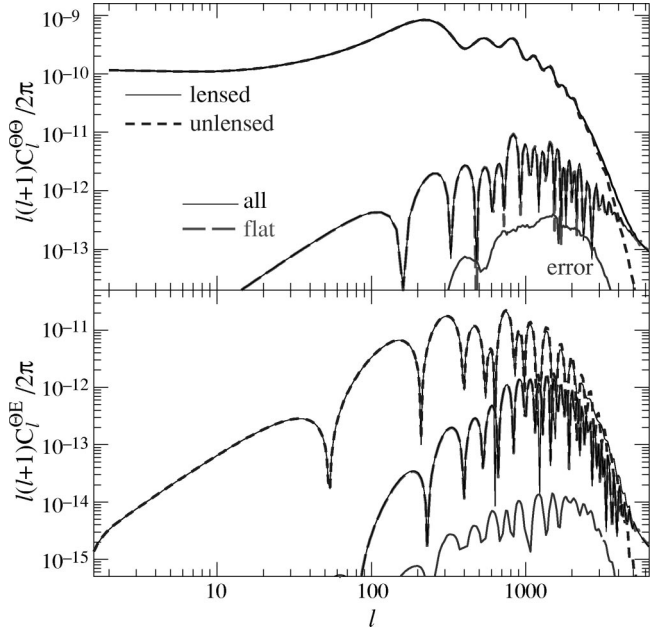


FIG. 1. Temperature and temperature-polarization cross power spectra. Shown here are the power spectra of the unlensed and lensed fields, their difference in the all-sky and flat-sky calculations and the error induced by using the flat sky expressions. The oscillatory nature of the difference indicates that lensing smooths the power spectrum.

For the bispectra, we have assumed that the triplet is composed of an even number of magnetic parity ( $B$ ) objects such that it vanishes for  $l+l'+l'' = \text{odd}$ . For combinations involving an odd number (e.g.,  $B\Theta\Theta$ ), the Wigner-3j symbol should be replaced with its algebraic approximation (B2) but with  $l+l'+l'' = \text{even}$  terms set to zero instead. However,

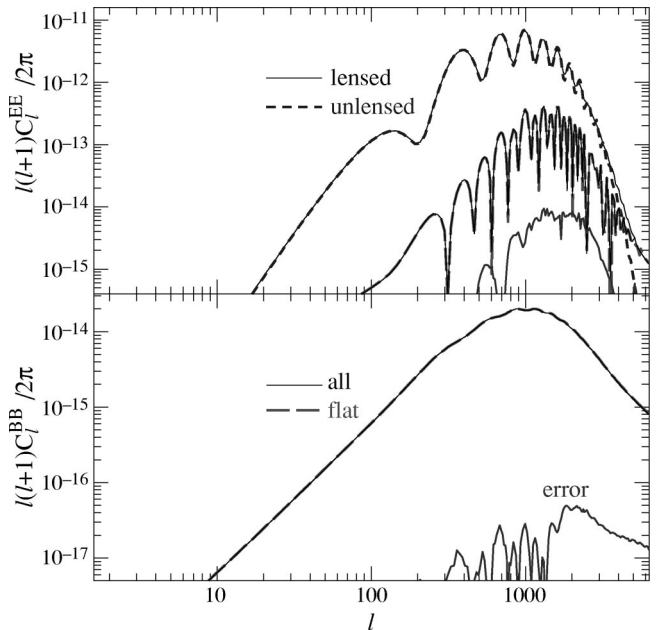


FIG. 2. Polarization power spectra. The same as in Fig. 1 except for the  $E$  and  $B$  polarization. We have assumed that the unlensed  $B$  spectrum vanishes as appropriate for scalar perturbations.

the overall sign depends on the orientation of the triangle in the flat-sky approximation since the bispectrum is then anti-symmetric to reflections about either axis.

### C. Weak lensing

In the so-called Born approximation where lensing effects are evaluated on the the null-geodesics of the unlensed photons, all effects can be conveniently encapsulated in the projected potential [14,15]

$$\phi(\hat{\mathbf{n}}) = -2 \int dD g_\phi(D) \Phi[\mathbf{x}(\hat{\mathbf{n}}), D], \quad (21)$$

where

$$g_\phi(D) = \frac{1}{D_A(D)} \int_D^\infty dD' \frac{D_A(D' - D)}{D_A(D')} g_s(D'). \quad (22)$$

For the CMB, the source distribution  $g_s$  is the Thomson visibility and may be replaced by a delta function at the last scattering surface  $D_s = D(z \sim 10^3)$ ; for galaxy weak lensing this is the distance distribution of the sources. We explicitly relate this quantity to the more familiar convergence and shear in Appendix A. Note that the deflection angle is given by the angular gradient  $\boldsymbol{\alpha}(\hat{\mathbf{n}}) = \nabla \phi(\hat{\mathbf{n}})$ .

As with the temperature perturbations, we can decompose the lensing potential into multipole moments

$$\phi(\hat{\mathbf{n}}) = \sum_{lm} \phi_{lm} Y_l^m(\hat{\mathbf{n}}), \quad (23)$$

or Fourier moments as

$$\phi(\hat{\mathbf{n}}) = \int \frac{d^2\mathbf{l}}{(2\pi)^2} \phi(\mathbf{l}) e^{i\mathbf{l} \cdot \hat{\mathbf{n}}}, \quad (24)$$

The power spectra of the lensing potential in the all-sky and flat-sky cases as

$$\begin{aligned} \langle \phi_{lm}^* \phi_{l'm'} \rangle &= \delta_{l,l'} \delta_{m,m'} C_l^{\phi\phi}, \\ \langle \phi^*(\mathbf{l}) \phi(\mathbf{l}') \rangle &= (2\pi)^2 \delta(\mathbf{l} - \mathbf{l}') C_{(l)}^{\phi\phi}, \end{aligned} \quad (25)$$

where again  $C_{(l)}^{\phi\phi} = C_l^{\phi\phi}$ . The lensing potential also develops a bispectrum in the nonlinear density regime

$$\begin{aligned} \langle \phi_{lm} \phi_{l'm'} \phi_{l''m''} \rangle &= \begin{pmatrix} l & l' & l'' \\ m & m' & m'' \end{pmatrix} B_{ll'l''}^{\phi\phi\phi}, \\ \langle \phi(\mathbf{l}) \phi(\mathbf{l}') \phi(\mathbf{l}'') \rangle &= (2\pi)^2 \delta(\mathbf{l} - \mathbf{l}' - \mathbf{l}'') B_{(l,l',l'')}^{XX'X''}, \end{aligned} \quad (26)$$

which is responsible for skewness in convergence maps and other higher order effects. Since the lensing potential is not affected by non-linearity until very high multipoles (see Fig. 3), we neglect these terms here.

Finally, the lensing potential can also be correlated with secondary temperature and polarization anisotropies [4,10], so that one must also consider the cross power spectra

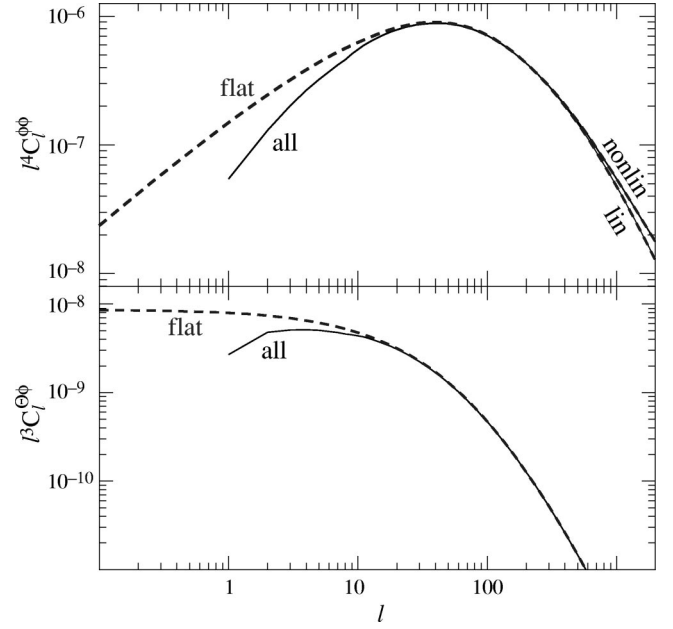


FIG. 3. Lensing power spectra. The power spectrum of the lensing potential is shown in the top panel as calculated by the flat and all sky approaches for linear and nonlinear density perturbations. In the lower panel, the cross correlation with the ISW effect is shown. In both cases, a non-negligible fraction of the power comes from scales where the flat-sky approximation is inadequate.

$$\begin{aligned} \langle X_{lm}^* \phi_{l'm'} \rangle &= \delta_{l,l'} \delta_{m,m'} C_l^{X\phi}, \\ \langle X^*(\mathbf{l}) \phi(\mathbf{l}') \rangle &= (2\pi)^2 \delta(\mathbf{l} - \mathbf{l}') C_{(l)}^{X\phi}, \end{aligned} \quad (27)$$

in the all and flat sky limits.

To calculate the power spectra of the lensing potential for a given cosmology one expands the gravitational potential in Eq. (21) in plane waves and then the plane waves in spherical harmonics. The result is

$$C_l^{\phi\phi} = 4\pi \int \frac{dk}{k} \Delta_\Phi^2(k, z) [I_l^{\text{len}}(k)]^2, \quad (28)$$

where

$$\begin{aligned} I_l^{\text{len}}(k) &= \int dD W^{\text{len}}(D) j_l\left(\frac{k}{H_0} D\right), \\ W^{\text{len}}(D) &= -2F(D) \frac{D_A(D_s - D)}{D_A(D) D_A(D_s)}. \end{aligned} \quad (29)$$

For curved universes, replace the spherical Bessel function with the ultraspherical Bessel function. In the small scale limit, this expression may be replaced by its equivalent Limber approximated integral [14]

$$C_{(l)}^{\phi\phi} = \frac{2\pi^2}{l^3} \int dD D_A [W^{\text{len}}(D)]^2 \Delta_\Phi^2(k, 0) |_{k=l(H_0/D_A)},$$

This expression also has the useful property that its nonlinear analogue can be calculated with the replacement

$$F(D)^2 \Delta_{\Phi}^2(k, 0) \rightarrow \Delta_{\Phi}^2(k, D), \quad (30)$$

where the time-dependent nonlinear power spectrum is given by the scaling formula [16] and the Poisson equation (5). Since nonlinear effects generally only appear at small angles, the full nonlinear all-sky spectrum can be obtained by matching these expressions in the linear regime (see Fig. 3).

Similarly, the cross correlation may be calculated for any secondary effect once its relation to the gravitational potential is known. We shall illustrate these results with the integrated Sachs-Wolfe effect. It contributes to temperature fluctuations as

$$\Theta^{\text{ISW}}(\hat{\mathbf{n}}) = -2 \int dD \dot{\Phi}[\mathbf{x}(\hat{\mathbf{n}}), D]. \quad (31)$$

It then follows that the all-sky cross correlation is given by [4,10]

$$C_l^{\Theta\phi} = 4\pi \int \frac{dk}{k} \Delta_{\Phi}^2(k) I_l^{\text{len}}(k) I_l^{\text{ISW}}(k), \quad (32)$$

where

$$I_l^{\text{ISW}}(k) = \int dD W^{\text{ISW}}(D) j_l\left(\frac{k}{H_0} D\right),$$

$$W^{\text{ISW}}(D) = -2\dot{F}(D), \quad (33)$$

again with the understanding that one replaces the spherical Bessel function with the ultra-spherical Bessel functions for curved universes. Similarly the flat-sky expression becomes

$$C_{(l)}^{\Theta\phi} = \frac{2\pi^2}{l^3} \int dD D_A W^{\text{ISW}}(D) W^{\text{len}}(D) \Delta_{\Phi}^2(k)|_{k=l(H_0/D_A)}.$$

Figure 3 also shows the cross-correlation for the  $\Lambda$ CDM cosmology.

Cross lensing-CMB bispectrum terms can also be included but require an external measure of lensing (e.g., a galaxy weak lensing survey) to be observable with three-point correlations.

### III. FLAT-SKY POWER SPECTRA

In this section, we calculate the effects of lensing on the CMB temperature (Sec. III A), polarization and cross (Sec. III B) power spectra. The simplicity of the resulting expressions have calculational and pedagogical advantages over the traditional flat-sky correlation function approach [2,3]. However we also show why one cannot expect a flat-sky approach to be fully accurate even on small scales.

#### A. Temperature

Weak lensing of the CMB remaps the primary anisotropy according to the deflection angle  $\nabla\phi$

$$\begin{aligned} \bar{\Theta}(\hat{\mathbf{n}}) &= \Theta(\hat{\mathbf{n}} + \nabla\phi) \\ &= \Theta(\hat{\mathbf{n}}) + \nabla_i \phi(\hat{\mathbf{n}}) \nabla^i \Theta(\hat{\mathbf{n}}) \\ &\quad + \frac{1}{2} \nabla_i \phi(\hat{\mathbf{n}}) \nabla_j \phi(\hat{\mathbf{n}}) \nabla^i \nabla^j \Theta(\hat{\mathbf{n}}) + \dots \end{aligned} \quad (34)$$

Because surface brightness is conserved, lensing only changes the distribution of the anisotropies and has no effect on the isotropic part of the background.

The Fourier coefficients of the lensed field then become

$$\bar{\Theta}(\mathbf{l}) = \int d\hat{\mathbf{n}} \bar{\Theta}(\hat{\mathbf{n}}) e^{-i\mathbf{l}\cdot\hat{\mathbf{n}}} = \Theta(\mathbf{l}) - \int \frac{d^2\mathbf{l}_1}{(2\pi)^2} \Theta(\mathbf{l}_1) L(\mathbf{l}, \mathbf{l}_1), \quad (35)$$

where

$$\begin{aligned} L(\mathbf{l}, \mathbf{l}_1) &= \phi(\mathbf{l} - \mathbf{l}_1) (\mathbf{l} - \mathbf{l}_1) \cdot \mathbf{l}_1 + \frac{1}{2} \int \frac{d^2\mathbf{l}_2}{(2\pi)^2} \phi(\mathbf{l}_2) \phi^*(\mathbf{l}_2 + \mathbf{l}_1 - \mathbf{l}) \\ &\quad \times (\mathbf{l}_2 \cdot \mathbf{l}_1) (\mathbf{l}_2 + \mathbf{l}_1 - \mathbf{l}) \cdot \mathbf{l}_1. \end{aligned} \quad (36)$$

This determines the lensed power spectrum

$$\langle \bar{\Theta}^*(\mathbf{l}) \bar{\Theta}(\mathbf{l}') \rangle = (2\pi)^2 \delta(\mathbf{l} - \mathbf{l}') \bar{C}_l^{\Theta\Theta}, \quad (37)$$

as

$$\bar{C}_l^{\Theta\Theta} = (1 - l^2 R) C_l^{\Theta\Theta} + \int \frac{d^2\mathbf{l}_1}{(2\pi)^2} C_{|\mathbf{l} - \mathbf{l}_1|}^{\Theta\Theta} C_{\mathbf{l}_1}^{\phi\phi} [(\mathbf{l} - \mathbf{l}_1) \cdot \mathbf{l}_1]^2, \quad (38)$$

where

$$R = \frac{1}{4\pi} \int \frac{dl}{l} l^4 C_l^{\phi\phi}. \quad (39)$$

The second term in Eq. (38) represents a convolution of the power spectra. Since  $l^4 C_l^{\phi\phi}$  peaks at low  $l$ 's compared with the peaks in the CMB (see Fig. 3), it can be considered as a narrow window function on  $C_l^{\Theta\Theta}$  in the acoustic regime  $200 \leq l \leq 2000$ . It is useful to consider the limit that  $C_l^{\Theta\Theta}$  is slowly varying. It may then be evaluated at  $\mathbf{l} - \mathbf{l}_1 \approx \mathbf{l}$  and taken out of the integral

$$C_l^{\Theta\Theta} \int \frac{d^2\mathbf{l}_1}{(2\pi)^2} C_l^{\phi\phi} (\mathbf{l} \cdot \mathbf{l}_1)^2 \approx l^2 R C_l^{\Theta\Theta}. \quad (40)$$

Note that the two terms in Eq. (37) cancel in this limit

$$\bar{C}_l^{\Theta\Theta} \approx C_l^{\Theta\Theta}. \quad (41)$$

This is the well known result that lensing shifts but does not create power on large scales. Intrinsic features with width  $\Delta l$  less than the  $l$  of the peak in  $l^4 C_l^{\phi\phi}$  are washed out by the convolution (see Fig. 3). Note that in the  $\Lambda$ CDM model this scale is  $l \sim 40$ . The implication is that for such a model, the

smoothing effect even for high multipoles arises from such low multipoles that the flat-sky approach is suspect.

On scales small compared with the damping length  $l \gtrsim 2000$ , there is little intrinsic power in the CMB so that the first term in Eq. (38) can be ignored and the second term behaves instead as a smoothing of  $C_l^{\phi\phi}$  of width  $\Delta l$  approximately the  $l$  of the peak in  $l^4 C_l^{\Theta\Theta}$ . Since  $C_l^{\phi\phi}$  is very smooth itself, the term is approximately

$$\tilde{C}_l^{\Theta\Theta} \approx C_l^{\Theta\Theta} + \frac{1}{2} l^2 C_l^{\phi\phi} \int \frac{d^2 \mathbf{l}_1}{(2\pi)^2} l_1^2 C_{l_1}^{\Theta\Theta}, \quad (42)$$

where we have interchanged the roles of  $\mathbf{l}_1$  and  $\mathbf{l}_1 - \mathbf{l}$ . The power generated is proportional to the lensing power at the same scale and may be approximated as the lensing of a pure temperature gradient [5]. In this limit the flat-sky approximation should be fully adequate.

### B. Polarization

The lensing of the polarization field may be obtained by following the same steps as for the temperature field

$$\begin{aligned} \pm \tilde{X}(\hat{\mathbf{n}}) &= \pm X(\hat{\mathbf{n}} + \nabla \phi) \\ &\approx \pm X(\hat{\mathbf{n}}) + \nabla_i \phi(\hat{\mathbf{n}}) \nabla_{\pm}^i X(\hat{\mathbf{n}}) \\ &\quad + \frac{1}{2} \nabla_i \phi(\hat{\mathbf{n}}) \nabla_j \phi(\hat{\mathbf{n}}) \nabla^i \nabla_{\pm}^j X(\hat{\mathbf{n}}), \end{aligned} \quad (43)$$

where we have used the shorthand notation  $\pm X = Q \pm iU$ . The Fourier coefficients of the lensed field are then

$$\pm \tilde{X}(\mathbf{l}) = \pm X(\mathbf{l}) - \int \frac{d^2 \mathbf{l}_1}{(2\pi)^2} \pm X(\mathbf{l}_1) e^{\pm 2i(\varphi_{l_1} - \varphi_l)} L(\mathbf{l}, \mathbf{l}_1), \quad (44)$$

where  $L$  was defined in Eq. (36).

Recalling that  $\pm X(\mathbf{l}) = E(\mathbf{l}) \pm iB(\mathbf{l})$ , we obtain the power spectra directly

$$\begin{aligned} \tilde{C}_l^{EE} &= (1 - l^2 R) C_l^{EE} + \frac{1}{2} \int \frac{d^2 \mathbf{l}_1}{(2\pi)^2} [(\mathbf{l} - \mathbf{l}_1) \cdot \mathbf{l}_1]^2 C_{|\mathbf{l} - \mathbf{l}_1|}^{\phi\phi} \\ &\quad \times [(C_{l_1}^{EE} + C_{l_1}^{BB}) + \cos(4\varphi_{l_1})(C_{l_1}^{EE} - C_{l_1}^{BB})], \\ \tilde{C}_l^{BB} &= (1 - l^2 R) C_l^{BB} + \frac{1}{2} \int \frac{d^2 \mathbf{l}_1}{(2\pi)^2} [(\mathbf{l} - \mathbf{l}_1) \cdot \mathbf{l}_1]^2 C_{|\mathbf{l} - \mathbf{l}_1|}^{\phi\phi} \\ &\quad \times [(C_{l_1}^{EE} + C_{l_1}^{BB}) - \cos(4\varphi_{l_1})(C_{l_1}^{EE} - C_{l_1}^{BB})], \\ \tilde{C}_l^{\Theta E} &= (1 - l^2 R) C_l^{\Theta E} + \int \frac{d^2 \mathbf{l}_1}{(2\pi)^2} \\ &\quad \times [(\mathbf{l} - \mathbf{l}_1) \cdot \mathbf{l}_1]^2 C_{|\mathbf{l} - \mathbf{l}_1|}^{\phi\phi} C_{l_1}^{\Theta E} \cos(2\varphi_{l_1}), \end{aligned} \quad (45)$$

where recall that  $R$  was defined in Eq. (39). The cross correlations between  $B$  and  $\Theta$  or  $E$  still vanish since lensing is

parity conserving. Unlike the case of the temperature fluctuations, lensing does not conserve the broadband large scale power of the  $E$  and  $B$  [3], but only the total polarization power. For example, lensing will create a  $B$  component in a field that originally had only an  $E$  component. Furthermore, lensing actually destroys temperature-polarization cross correlations due to the lack of correlation with the generated  $B$  polarization. From Fig. 1, one can see that the largest relative effect of lensing is on the correlation.

## IV. ALL-SKY POWER SPECTRA

In this section, we treat lensing effects on the temperature (Sec. IV A), polarization and cross (Sec. IV B) power spectra in a full all-sky formalism. Corrections to the flat-sky results remain at the 10% even on small scales. Moreover, although the derivation appears more complicated, the end results for the power spectra are simple. They are as readily evaluated as the flat-sky counterparts and should be used in their stead.

### A. Temperature

In the all-sky case, the Fourier harmonics are replaced with spherical harmonics, and the lensed field becomes

$$\begin{aligned} \tilde{\Theta}_{lm} &\approx \Theta_{lm} + \int d\hat{\mathbf{n}} Y_l^{m*} \nabla_i \phi(\hat{\mathbf{n}}) \nabla^i \Theta(\hat{\mathbf{n}}) \\ &\quad + \frac{1}{2} \int d\hat{\mathbf{n}} Y_l^{m*} \nabla_i \phi(\hat{\mathbf{n}}) \nabla_j \phi(\hat{\mathbf{n}}) \nabla^i \nabla^j \Theta(\hat{\mathbf{n}}) \\ &= \Theta_{lm} + \sum_{l_1 m_1} \sum_{l_2 m_2} \phi_{l_1 m_1} \Theta_{l_2 m_2} \\ &\quad \times \left[ I_{ll_1 l_2}^{mm_1 m_2} + \frac{1}{2} \sum_{l_3 m_3} \phi_{l_3 m_3}^* J_{ll_1 l_2 l_3}^{mm_1 m_2 m_3} \right], \end{aligned} \quad (46)$$

with the geometrical factors expressed as integrals over the spherical harmonics

$$\begin{aligned} I_{ll_1 l_2}^{mm_1 m_2} &= \int d\hat{\mathbf{n}} Y_l^{m*} (\nabla_i Y_{l_1}^{m_1}) (\nabla^i Y_{l_2}^{m_2}), \\ J_{ll_1 l_2 l_3}^{mm_1 m_2 m_3} &= \int d\hat{\mathbf{n}} Y_l^{m*} (\nabla_i Y_{l_1}^{m_1}) (\nabla_j Y_{l_3}^{m_3}) \nabla^i \nabla^j Y_{l_2}^{m_2}. \end{aligned} \quad (47)$$

The lensed power spectrum then becomes

$$\tilde{C}_l = C_l + \sum_{l_1 l_2} C_{l_1}^{\phi\phi} C_{l_2}^{\Theta\Theta} S_1 + C_l^{\Theta\Theta} \sum_{l_1} C_{l_1}^{\phi\phi} S_2, \quad (48)$$

with

$$\begin{aligned} S_1 &= \sum_{m_1 m_2} (I_{ll_1 l_2}^{mm_1 m_2})^2, \\ S_2 &= \frac{1}{2} \sum_{m_1} J_{ll_1 l_1}^{mm_1 m m_1} + \text{c.c.}, \end{aligned} \quad (49)$$

where c.c. denotes the complex conjugate and we have suppressed the  $l$  indices.

These formidable looking expressions simplify considerably. The second term may be rewritten through integration by parts and the identity  $\nabla^2 Y_l^m = -l(l+1)Y_l^m$  [4],

$$I_{l_1 l_2}^{m_1 m_2} = \frac{1}{2} [l_1(l_1+1) + l_2(l_2+1) - l(l+1)] \int d\hat{\mathbf{n}} Y_l^{m_1*} Y_{l_1}^{m_1} Y_{l_2}^{m_2}. \quad (50)$$

The remaining integral may be expressed in terms of the Wigner-3j symbol through the general relation

$$\begin{aligned} & \int d\hat{\mathbf{n}} ({}_{s_1} Y_{l_1}^{m_1*})_{s_2} Y_{l_2}^{m_2} ({}_{s_3} Y_{l_3}^{m_3}) \\ &= (-1)^{m_1+s_1} \sqrt{\frac{(2l_1+1)(2l_2+1)(2l_3+1)}{4\pi}} \\ & \times \begin{pmatrix} l_1 & l_2 & l_3 \\ s_1 & -s_2 & -s_3 \end{pmatrix} \begin{pmatrix} l_1 & l_2 & l_3 \\ -m_1 & m_2 & m_3 \end{pmatrix}, \quad (51) \end{aligned}$$

where note that  ${}_0 Y_l^m = Y_l^m$ . It is therefore convenient to define

$$\begin{aligned} F_{l_1 l_2 l_3} &= \frac{1}{2} [l_2(l_2+1) + l_3(l_3+1) - l_1(l_1+1)] \\ & \times \sqrt{\frac{(2l_1+1)(2l_2+1)(2l_3+1)}{4\pi}} \begin{pmatrix} l_1 & l_2 & l_3 \\ 0 & 0 & 0 \end{pmatrix}. \quad (52) \end{aligned}$$

Finally the Wigner-3j symbol obeys

$$\sum_{m_1 m_2} \begin{pmatrix} l_1 & l_2 & l_3 \\ m_1 & m_2 & m_3 \end{pmatrix} \begin{pmatrix} l_1 & l_2 & l_3 \\ m_1 & m_2 & m_3 \end{pmatrix} = \frac{1}{2l_3+1}. \quad (53)$$

Putting these relations together, we find that

$$S_1 = \frac{1}{2l+1} (F_{l l_1 l_2})^2. \quad (54)$$

An algebraic expression for the relevant Wigner-3j symbol is given in Appendix B.

The second term in Eq. (48) can be simplified by re-expressing the gradients of the spherical harmonics with spin-1 spherical harmonics. As shown in Appendix A, the spin-1 harmonics are the eigenmodes of vector fields on the sky and naturally appear in expressions for deflection angles. Note that there is a general relation for raising and lowering the spin of a spherical harmonic [11]

$$\begin{aligned} \mathbf{m}_- \cdot \nabla_s Y_l^m &= \sqrt{\frac{(l-s)(l+s+1)}{2}} {}_{s+1} Y_l^m, \\ \mathbf{m}_+ \cdot \nabla_s Y_l^m &= -\sqrt{\frac{(l+s)(l-s+1)}{2}} {}_{s-1} Y_l^m, \quad (55) \end{aligned}$$

so that

$$\nabla Y_l^m = \sqrt{\frac{l(l+1)}{2}} [{}_1 Y_l^m \mathbf{m}_+ - {}_{-1} Y_l^m \mathbf{m}_-]. \quad (56)$$

As an aside, we note that Eq. (54) can alternately be derived from this relation and the integral (51) with  $s = \pm 1$ .

Further, we note that spin spherical harmonics also obey a sum rule [17]

$$\sum_m {}_{s_1} Y_l^{m*}(\hat{\mathbf{n}}) {}_{s_2} Y_l^m(\hat{\mathbf{n}}) = \sqrt{\frac{2l+1}{4\pi}} {}_{s_2} Y_l^{-s_1}(\mathbf{0}). \quad (57)$$

For the spin-1 harmonics

$${}_{-1} Y_l^1(\mathbf{0}) = {}_1 Y_l^{-1}(\mathbf{0}) = -\sqrt{\frac{2l+1}{4\pi}}, \quad (58)$$

and the others involving  $s_1, s_2 = \pm 1$  vanish. These results imply that

$$\begin{aligned} \sum_m \nabla_i Y_l^m \nabla_j Y_l^{m*} &= \frac{1}{2} l(l+1) \frac{2l+1}{4\pi} [(\mathbf{m}_+)_i (\mathbf{m}_-)_j \\ & + (\mathbf{m}_-)_i (\mathbf{m}_+)_j]. \quad (59) \end{aligned}$$

To evaluate the second derivative term in Eq. (47), we again apply Eq. (55) to show that

$$\begin{aligned} & [(\mathbf{m}_+)_i (\mathbf{m}_-)_j + (\mathbf{m}_-)_i (\mathbf{m}_+)_j] \nabla^i \nabla^j {}_s Y_l^m \\ &= -[l(l+1) - s^2] {}_s Y_l^m. \quad (60) \end{aligned}$$

Putting these expressions together we obtain

$$S_2 = -\frac{1}{2} l(l+1) l_1(l_1+1) \frac{2l_1+1}{4\pi}. \quad (61)$$

Finally combining expressions Eqs. (48), (54), and (61), we have the following simple result:

$$\tilde{C}_l^{\theta\theta} = [1 - l(l+1)R] C_l^{\theta\theta} + \sum_{l_1, l_2} C_{l_1}^{\phi\phi} C_{l_2}^{\phi\phi} \frac{(F_{l l_1 l_2})^2}{2l+1}, \quad (62)$$

where

$$R = \frac{1}{2} \sum_{l_1} l_1(l_1+1) \frac{2l_1+1}{4\pi} C_{l_1}^{\phi\phi}. \quad (63)$$

This expression is computationally no more involved than the flat-sky expression Eq. (38) and has the benefit of being exact. Since the lensing effect even at high  $l$  in the CMB originates from the low order multipoles of  $\phi$ , corrections due to the curvature of the sky are not confined to low  $l$ . We show in Fig. 1 that the correction causes a 10% difference in the effect. The change in  $\tilde{C}_l^{\theta\theta}$  itself is even smaller (of order 1%). Nonetheless it is larger than the cosmic variance of these high multipoles and thus should be included in calcu-

lations for full accuracy. Corrections can be even larger in models with a red tilt  $n < 1$  in the initial spectrum.

### B. Polarization

The derivation of the all-sky generalization for polarization is superficially more involved but follows the same steps as in the temperature case and results in expressions that are no more difficult to evaluate. The lensed polarization multipoles are given by

$$\begin{aligned} \pm X_{lm} &= \pm X_{lm} + \sum_{l_1 m_1} \sum_{l_2 m_2} \phi_{l_1 m_1 \pm X_{l_2 m_2}} \\ &\times \left[ \pm 2 I_{ll_1 l_2}^{mm_1 m_2} + \frac{1}{2} \sum_{l_3 m_3} \phi_{l_3 m_3}^* \pm 2 J_{ll_1 l_2 l_3}^{mm_1 m_2 m_3} \right], \end{aligned} \quad (64)$$

with the geometrical factors expressed now as integrals over the spin-spherical harmonics

$$\begin{aligned} \pm 2 I_{ll_1 l_2}^{mm_1 m_2} &= \int d\hat{\mathbf{n}}_{\pm 2} Y_{l_1}^{m_1*} (\nabla_i Y_{l_1}^{m_1}) (\nabla^i \pm 2 Y_{l_2}^{m_2}), \\ \pm 2 J_{ll_1 l_2 l_3}^{mm_1 m_2 m_3} &= \int d\hat{\mathbf{n}}_{\pm 2} Y_{l_1}^{m_1*} (\nabla_i Y_{l_1}^{m_1}) (\nabla_i Y_{l_3}^{m_3*}) (\nabla^i \nabla^j \pm 2 Y_{l_2}^{m_2}). \end{aligned} \quad (65)$$

Noting that

$$\pm 2 I_{ll_1 l_2}^{mm_1 m_2} = (-1)^L \mp 2 I_{ll_1 l_2}^{mm_1 m_2}, \quad (66)$$

where  $L = l + l_1 + l_2$  and recalling that  $\pm X_{lm} = E_{lm} \pm i B_{lm}$ , the power spectra then become

$$\begin{aligned} \tilde{C}_l^{EE} &= C_l^{EE} + \frac{1}{2} \sum_{l_1 l_2} C_{l_1}^{\phi\phi} [(C_{l_2}^{EE} + C_{l_2}^{BB}) + (-1)^L \\ &\times (C_{l_2}^{EE} - C_{l_2}^{BB})]_{22} S_1 + \frac{1}{2} C_l^{EE} \sum_{l_1} C_{l_1}^{\phi\phi} ({}_2 S_2 + {}_{-2} S_2), \end{aligned} \quad (67)$$

where

$$\begin{aligned} {}_{22} S_1 &= \sum_{m_1 m_2} ({}_2 I_{ll_1 l_2}^{mm_1 m_2})^2, \\ {}_{\pm 2} S_2 &= \frac{1}{2} \sum_{m_1} \pm 2 J_{ll_1 l_1 l_1}^{mm_1 m_1 m_1} + \text{c.c.} \end{aligned} \quad (68)$$

The expression for  $\tilde{C}_l^{BB}$  follows by interchanging  $EE$  and  $BB$ . The cross power spectrum is

$$\begin{aligned} \tilde{C}_l^{\Theta E} &= C_l^{\Theta E} + \frac{1}{2} \sum_{l_1 l_2} C_{l_1}^{\phi\phi} C_{l_2}^{\Theta E} [1 + (-1)^L] {}_{02} S_1 \\ &+ \frac{1}{4} C_l^{\Theta E} \sum_{l_1} C_{l_1}^{\phi\phi} ({}_2 S_2 + {}_{-2} S_2 + 2 S_2), \end{aligned} \quad (69)$$

with

$${}_{02} S_1 = \sum_{m_1 m_2} (I_{ll_1 l_2}^{mm_1 m_2} {}_2 I_{ll_1 l_2}^{mm_1 m_2}). \quad (70)$$

Just as in the case for the temperature field, these expressions simplify considerably. The spin-2 harmonics are eigenfunctions of the angular Laplacian of a tensor

$$\nabla^2 \pm 2 Y_l^m = [-l(l+1) + 4] \pm 2 Y_l^m, \quad (71)$$

which follows from contracting indices in Eq. (60). It then follows that

$$\begin{aligned} \pm 2 I_{ll_1 l_2}^{mm_1 m_2} &= \frac{1}{2} [l_1(l_1+1) + l_2(l_2+1) \\ &- l(l+1)] \int d\hat{\mathbf{n}} (\pm 2 Y_{l_1}^{m_1*}) Y_{l_1}^{m_1} (\pm 2 Y_{l_2}^{m_2}). \end{aligned} \quad (72)$$

Comparison with Eq. (51) implies that it is convenient then to define the quantity

$$\begin{aligned} {}_2 F_{l_1 l_2 l_3} &= \frac{1}{2} [l_2(l_2+1) + l_3(l_3+1) - l_1(l_1+1)] \\ &\times \sqrt{\frac{(2l_1+1)(2l_2+1)(2l_3+1)}{4\pi}} \begin{pmatrix} l_1 & l_2 & l_3 \\ 2 & 0 & -2 \end{pmatrix}, \end{aligned} \quad (73)$$

so that

$$\begin{aligned} {}_{22} S_1 &= \frac{1}{2l+1} ({}_2 F_{ll_1 l_2})^2, \\ {}_{02} S_1 &= \frac{1}{2l+1} (F_{ll_1 l_2}) ({}_2 F_{ll_1 l_2}). \end{aligned} \quad (74)$$

The third term in Eq. (68) can be simplified by following the same steps for the analogous temperature term except for the replacement of  $s=0$  with  $s=\pm 2$  in Eq. (55). The result is

$$\pm 2 S_2 = -\frac{1}{2} [l(l+1) - 4] l_1(l_1+1) \frac{2l_1+1}{4\pi}. \quad (75)$$

Putting these relations together, we obtain the result for the power spectra

$$\begin{aligned} \tilde{C}_l^{EE} &= [1 - (l^2 + l - 4)R] C_l^{EE} + \frac{1}{2} \sum_{l_1 l_2} C_{l_1}^{\phi\phi} \frac{({}_2 F_{ll_1 l_2})^2}{2l+1} \\ &\times [C_{l_2}^{EE} + C_{l_2}^{BB} + (-1)^L (C_{l_2}^{EE} - C_{l_2}^{BB})], \\ \tilde{C}_l^{BB} &= [1 - (l^2 + l - 4)R] C_l^{BB} + \frac{1}{2} \sum_{l_1 l_2} C_{l_1}^{\phi\phi} \frac{({}_2 F_{ll_1 l_2})^2}{2l+1} \\ &\times [C_{l_2}^{EE} + C_{l_2}^{BB} - (-1)^L (C_{l_2}^{EE} - C_{l_2}^{BB})], \end{aligned}$$

$$\begin{aligned} \tilde{C}_l^{\Theta E} &= [1 - (l^2 + l - 2)R] C_l^{\Theta E} \\ &+ \sum_{l_1, l_2} C_{l_1}^{\phi\phi} \frac{(F_{ll_1 l_2} F_{ll_1 l_2})}{2l+1} C_{l_2}^{\Theta E}. \end{aligned} \quad (76)$$

Recall that  $L = l + l_1 + l_2$  and  $R$  was defined in Eq. (63). These expressions are plotted for the  $\Lambda$ CDM model in Fig. 2.

## V. FLAT- AND ALL-SKY BISPECTRA

In this section, we consider the lensing contributions to CMB bispectra through the correlation with secondary anisotropies. We begin by reviewing the calculations for the temperature bispectrum as previously treated by Refs. [4,5]. We then introduce the polarization and cross bispectra which in principle have signal-to-noise advantages over the temperature bispectra. We illustrate the formalism with a concrete calculation of the effect due to the ISW secondary anisotropy.

### A. Temperature

Contributions to the temperature bispectra from the cross power spectrum  $C_l^{\Theta\phi}$  discussed in Sec. II C follow immediately from the first order lensing term, i.e., Eq. (46) for the all-sky bispectrum [4],

$$B_{l_1 l_2 l_3}^{\Theta\Theta\Theta} = F_{l_1 l_2 l_3} C_{l_2}^{\Theta\phi} C_{l_3}^{\Theta\Theta} + 5 \text{ perm}, \quad (77)$$

and Eq. (35) for the flat sky bispectrum [5]

$$B_{(\mathbf{l}_1, \mathbf{l}_2, \mathbf{l}_3)}^{\Theta\Theta\Theta} = -(\mathbf{l}_2 \cdot \mathbf{l}_3) C_{l_2}^{\Theta\phi} C_{l_3}^{\Theta\Theta} + 5 \text{ perm} \quad (78)$$

One can show that these relations satisfy the general expression for the correspondence between flat and all sky bispectra Eq. (20) by noting that

$$\mathbf{l}_2 \cdot \mathbf{l}_3 = -\frac{1}{2}(l_2^2 + l_3^2 - l_1^2), \quad (79)$$

since the angles of a triangle is fully defined by the length of its sides.

Note that there can be strong cancellation between the terms in the permutation in both cases. As we have seen, the spectrum of  $\phi$  is generally peaked to low multipoles implying a corresponding weighting of  $C_l^{\Theta\phi}$  to low multipoles for secondary anisotropies that correlate strongly with  $\phi$ . In this case the triangles  $(l_1, l_2, l_3)$  that contribute most strongly are highly flattened such that two sides nearly coincide in length  $l_1 \approx l_3 \gg l_2$ . In this case, contributions  $l_1^2$  and  $l_3^2$  in Eq. (79) are cancelled off the permutation  $\mathbf{l}_3 \leftrightarrow \mathbf{l}_1$  leaving only a term of order  $l_2^2$ .

These considerations also signal problems for the flat-sky expressions. It is important to know what on scales most of the detectable signal is coming from. In the all-sky formalism, the signals from the  $m$  modes are added together with weights given by the Wigner-3j symbol

$$B_{l_1 l_2 l_3}^{\Theta\Theta\Theta} = \sum_{m_1 m_2 m_3} \begin{pmatrix} l_1 & l_2 & l_3 \\ m_1 & m_2 & m_3 \end{pmatrix} \langle \Theta_{l_1 m_1} \Theta_{l_2 m_2} \Theta_{l_3 m_3} \rangle. \quad (80)$$

For the small effects due to the correlation of secondary anisotropies with lensing, the covariance of the bispectrum estimators is dominated by the Gaussian noise from the power spectrum [18]

$$\text{Cov} = C_{l_1}^{\Theta\Theta} C_{l_2}^{\Theta\Theta} C_{l_3}^{\Theta\Theta} \delta_{l_1 l_1'} \delta_{l_2 l_2'} \delta_{l_3 l_3'} + 5 \text{ perm}, \quad (81)$$

where the permutations are in the indices of the  $l'$  triplet. The overall signal-to-noise becomes

$$\left(\frac{S}{N}\right)^2 = \sum_{l_1 l_2 l_3} \sum_{l_1' l_2' l_3'} B_{l_1 l_2 l_3}^{\Theta\Theta\Theta} [\text{Cov}^{-1}] B_{l_1' l_2' l_3'}^{\Theta\Theta\Theta}. \quad (82)$$

The covariance is in general diagonal in the  $6 \times 6$  blocks of permutations of  $(l_1, l_2, l_3)$  and for this simple case of the temperature bispectrum, the blocks are proportional to the trivial matrix of all ones. The result is one can take a simple sum over all distinct triplets or equivalently divide the full sum by a factor of 6,

$$\left(\frac{S}{N}\right)^2 = \sum_{l_1 l_2 l_3} \frac{(B_{l_1 l_2 l_3}^{\Theta\Theta\Theta})^2}{6 C_{l_1}^{\Theta\Theta} C_{l_2}^{\Theta\Theta} C_{l_3}^{\Theta\Theta}}, \quad (83)$$

for a cosmic variance limited experiment. For a realistic experiment with noise from the detectors and residual foregrounds, one simply replaces

$$C_l^{XX'} \rightarrow C_l^{XX'} + C_l^{XX'}(\text{noise}), \quad (84)$$

here and below. Note that one can also construct the Fisher information matrix of the bispectrum along these lines [19].

Correspondingly, in the flat-sky approximation one constructs the optimal inverse-variance weighted statistic [5] (see also Appendix C)

$$\left(\frac{S}{N}\right)^2 = \frac{f_{\text{sky}}}{\pi} \frac{1}{(2\pi)^2} \int d^2 l_1 \int d^2 l_2 \frac{[B_{(l_1, l_2, l_3)}^{\Theta\Theta\Theta}]^2}{6 C_{l_1}^{\Theta\Theta} C_{l_2}^{\Theta\Theta} C_{l_3}^{\Theta\Theta}}, \quad (85)$$

where  $f_{\text{sky}}$  is the fraction of the sky covered. We show that these expressions are equivalent in the high  $l$ ,  $f_{\text{sky}} = 1$  limit in Appendix C. Thus the extra factor of  $f_{\text{sky}}$  can be included in the all-sky expression to approximate the effects incomplete sky coverage due to exclusion of regions contaminated by galactic foregrounds.

The weighting of the modes is such that the quantity of interest in the lensing-temperature correlation is  $l^3 C_l^{\Theta\phi}$  where the extra factor of  $l$  over the straight bispectrum contribution comes from the square root of the volume factor in  $l$  space. This quantity is plotted in Fig. 3 for the cross correlation with the ISW effect. The implication is that for this effect, full accuracy requires an all-sky approach and we shall hereafter use this to evaluate the signal-to-noise.

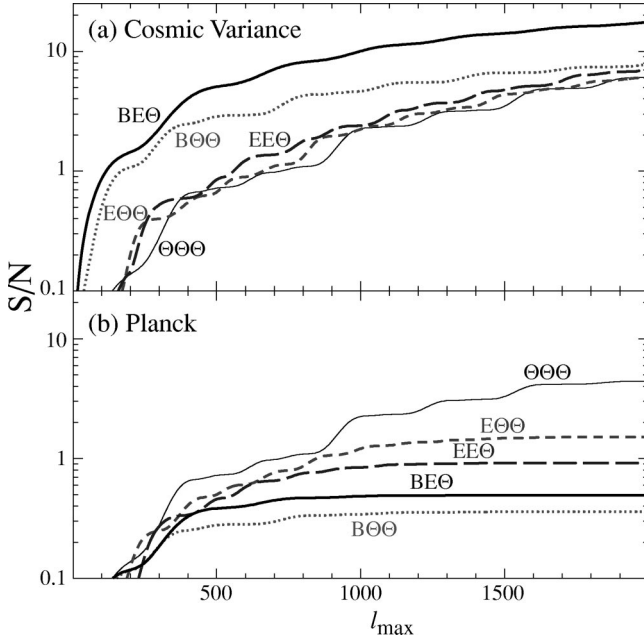


FIG. 4. Cumulative signal-to-noise in the bispectra as a function of maximum  $l$  for a cosmic variance limited experiment and for the Planck satellite. Note that for the cosmic variance limited case (a), bispectra involving the  $B$  polarization have a substantial signal-to-noise advantage over the other bispectra. For the Planck satellite (b), we assume that the additional variance comes only from detector noise. In practice, residual foreground contamination and sky cuts to avoid them will lower the signal-to-noise further.

The overall signal-to-noise as a function of the largest  $l$  included in the sum is shown in Fig. 4 for a cosmic variance limited experiment and the Planck satellite (see Ref. [19] for the specification of the noise). Note that the Planck satellite is effectively cosmic variance limited to  $l \sim 1000$  and even so the  $S/N$  is only of order a few [4].

### B. Polarization and cross correlation

Bispectra involving the  $E$  and  $B$  parity polarization will also receive contributions from the correlation induced by lensing. Although these signals are smaller than the temperature bispectrum in an absolute sense, we have seen that the main obstacle in detecting the temperature bispectrum is cosmic variance from the Gaussian contributions.

We begin by analyzing terms that do not involve the  $B$ -parity polarization. For these all-sky bispectra, only terms with  $L \equiv l_1 + l_2 + l_3 = \text{even}$  are nonvanishing, and we will implicitly assume that only even terms are considered. With the help of Eqs. (44) and (65), we can immediately write the all and flat sky results as

$$\begin{aligned}
 B_{l_1 l_2 l_3}^{E\Theta\Theta} &= {}_2F_{l_1 l_2 l_3} C_{l_2}^{\Theta\phi} C_{l_3}^{\Theta E} + F_{l_2 l_1 l_3} (C_{l_1}^{E\phi} C_{l_3}^{\Theta\Theta} + C_{l_1}^{\Theta E} C_{l_3}^{\Theta\phi}) \\
 &\quad + (l_2 \leftrightarrow l_3), \\
 B_{(l_1, l_2, l_3)}^{E\Theta\Theta} &= -(\mathbf{l}_2 \cdot \mathbf{l}_3) \cos 2\varphi_{31} C_{l_2}^{\Theta\phi} C_{l_3}^{\Theta E} - (\mathbf{l}_1 \cdot \mathbf{l}_3) \\
 &\quad \times (C_{l_1}^{E\phi} C_{l_3}^{\Theta\Theta} + C_{l_1}^{\Theta E} C_{l_3}^{\Theta\phi}) + (\mathbf{l}_2 \leftrightarrow \mathbf{l}_3), \quad (86)
 \end{aligned}$$

where

$$\varphi_{AB} = \varphi_{l_A} - \varphi_{l_B}. \quad (87)$$

The general correspondence between the flat and all sky expressions in Eq. (20) is established by the use of Eq. (79) the approximation discussed in Appendix B.

$$\begin{pmatrix} l_1 & l_2 & l_3 \\ 2 & 0 & -2 \end{pmatrix} \approx \cos 2\varphi_{31} \begin{pmatrix} l_1 & l_2 & l_3 \\ 0 & 0 & 0 \end{pmatrix}, \quad (88)$$

for  $L = \text{even}$ . The cancellation for flattened triangles discussed in Sec. V A still applies and is easiest to see in the flat-sky limit: the flatness of the triangles implies  $\cos 2\varphi_{31} \sim 1$ .

For the  $S/N$  calculation, note that the covariance is given by

$$\begin{aligned}
 \text{Cov} &= C_{l_1}^{EE} C_{l_2}^{\Theta\Theta} C_{l_3}^{\Theta\Theta} \delta_{l_1 l_1'} \delta_{l_2 l_2'} \delta_{l_3 l_3'} \\
 &\quad + C_{l_1}^{\Theta E} C_{l_2}^{\Theta\Theta} C_{l_3}^{\Theta E} \delta_{l_1 l_2'} \delta_{l_2 l_3'} \delta_{l_3 l_1'} \\
 &\quad + C_{l_1}^{\Theta E} C_{l_2}^{\Theta E} C_{l_3}^{\Theta\Theta} \delta_{l_1 l_3'} \delta_{l_2 l_1'} \delta_{l_3 l_2'} + (l_2 \leftrightarrow l_3'), \quad (89)
 \end{aligned}$$

so that a full calculation requires inverting this matrix for each distinct triplet. Since we are interested mainly in the order of magnitude of  $S/N$ , we can set the lower bound as

$$\left(\frac{S}{N}\right)^2 \geq \sum_{l_1 l_2 l_3} \frac{(B_{l_1 l_2 l_3}^{E\Theta\Theta})^2}{6 C_{l_1}^{EE} C_{l_2}^{\Theta\Theta} C_{l_3}^{\Theta\Theta}}, \quad (90)$$

which amounts to ignoring duplicate triplets and replacing the remaining triplet with the average  $S/N$  of the set. This limit is plotted for the ISW effect in Fig. 4 as a function of the maximal  $l_1$  included in the sum. As expected, it is comparable to the signal-to-noise in the temperature bispectrum. Of course, it is experimentally more difficult to achieve the cosmic variance limit in the polarization with a realistic experiment containing detector and foreground noise.

There is also a qualitatively new effect from the polarization-lensing correlation  $C_l^{E\phi}$ . However, since secondary polarization only arises from Thomson scattering effects, we expect this contribution to be small in  $\Lambda$ CDM models where the optical depth during reionization is  $\tau < 0.3$  [19].

The  $EE\Theta$  bispectrum term is

$$\begin{aligned}
 B_{l_1 l_2 l_3}^{EE\Theta} &= ({}_2F_{l_1 l_2 l_3} C_{l_2}^{E\phi} C_{l_3}^{\Theta E} + {}_2F_{l_1 l_3 l_2} C_{l_2}^{EE} C_{l_3}^{\Theta\phi}) \\
 &\quad + F_{l_3 l_1 l_2} C_{l_1}^{E\phi} C_{l_2}^{\Theta E} + (l_1 \leftrightarrow l_2), \\
 B_{(l_1, l_2, l_3)}^{EE\Theta} &= -(\mathbf{l}_2 \cdot \mathbf{l}_3) (\cos 2\varphi_{31} C_{l_2}^{E\phi} C_{l_3}^{\Theta E} \\
 &\quad + \cos 2\varphi_{21} C_{l_2}^{EE} C_{l_3}^{\Theta\phi}) - (\mathbf{l}_1 \cdot \mathbf{l}_2) C_{l_1}^{E\phi} C_{l_2}^{\Theta E} \\
 &\quad + (\mathbf{l}_1 \leftrightarrow \mathbf{l}_2), \quad (91)
 \end{aligned}$$

with covariance

$$\begin{aligned} \text{Cov} = & C_{l_1}^{EE} C_{l_2}^{EE} C_{l_3}^{\Theta\Theta} \delta_{l_1 l'_1} \delta_{l_2 l'_2} \delta_{l_3 l'_3} \\ & + C_{l_1}^{EE} C_{l_2}^{E\Theta} C_{l_3}^{\Theta E} \delta_{l_1 l'_1} \delta_{l_2 l'_2} \delta_{l_3 l'_1} \\ & + C_{l_1}^{\Theta E} C_{l_2}^{EE} C_{l_3}^{\Theta E} \delta_{l_1 l'_1} \delta_{l_2 l'_1} \delta_{l_3 l'_2} + (l'_1 \leftrightarrow l'_2), \end{aligned} \quad (92)$$

$$\left(\frac{S}{N}\right)^2 = \sum_{l_1 l_2 l_3} \frac{(B_{l_1 l_2 l_3}^{B\Theta\Theta})^2}{2 C_{l_1}^{BB} C_{l_2}^{EE} C_{l_3}^{\Theta\Theta}}. \quad (100)$$

with which we can bound the  $S/N$

$$\left(\frac{S}{N}\right)^2 > \sum_{l_1 l_2 l_3} \frac{(B_{l_1 l_2 l_3}^{EEE})^2}{6 C_{l_1}^{EE} C_{l_2}^{EE} C_{l_3}^{\Theta\Theta}}. \quad (93)$$

Again, the ISW example is shown in Fig. 4.

Finally the  $EEE$  bispectrum is given by

$$\begin{aligned} B_{l_1 l_2 l_3}^{EEE} = & {}_2F_{l_1 l_2 l_3} C_{l_2}^{E\phi} C_{l_3}^{EE} + 5 \text{ perm}, \\ B_{(l_1, l_2, l_3)}^{EEE} = & -(\mathbf{l}_2 \cdot \mathbf{l}_3) \cos 2\varphi_{31} C_{l_2}^{E\phi} C_{l_3}^{EE} + 5 \text{ perm}, \end{aligned} \quad (94)$$

with covariance

$$\text{Cov} = C_{l_1}^{EE} C_{l_2}^{EE} C_{l_3}^{EE} \delta_{l_1 l'_1} \delta_{l_2 l'_2} \delta_{l_3 l'_3} + 5 \text{ perm}, \quad (95)$$

and signal-to-noise

$$\left(\frac{S}{N}\right)^2 = \sum_{l_1 l_2 l_3} \frac{(B_{l_1 l_2 l_3}^{EEE})^2}{6 C_{l_1}^{EE} C_{l_2}^{EE} C_{l_3}^{EE}}. \quad (96)$$

This bispectrum signal vanishes for the ISW effect.

Bispectra involving the  $B$ -parity polarization have distinct properties. For terms involving one  $B$ -parity polarization term, only  $l_1 + l_2 + l_3 = \text{odd}$  contributes to the all-sky spectrum and we implicitly assume below that even terms vanish.

For the  $B\Theta\Theta$  bispectrum,

$$\begin{aligned} B_{l_1 l_2 l_3}^{B\Theta\Theta} = & i({}_2F_{l_1 l_2 l_3} C_{l_2}^{\Theta\phi} C_{l_3}^{\Theta E} + (l_2 \leftrightarrow l_3)), \\ B_{(l_1, l_2, l_3)}^{B\Theta\Theta} = & -(\mathbf{l}_2 \cdot \mathbf{l}_3) \sin 2\varphi_{31} C_{l_2}^{\Theta\phi} C_{l_3}^{\Theta E} - (\mathbf{l}_2 \leftrightarrow \mathbf{l}_3). \end{aligned} \quad (97)$$

Again the correspondence between the flat and all sky expressions in Eq. (20) is established by the approximation discussed in Appendix B

$$\begin{pmatrix} l_1 & l_2 & l_3 \\ 2 & 0 & -2 \end{pmatrix} \approx \pm i \sin 2\varphi_{31} \begin{pmatrix} l_1 & l_2 & l_3 \\ 0 & 0 & 0 \end{pmatrix}, \quad (98)$$

for  $L = \text{odd}$ . The sign ambiguity comes from the fact that a reflection of the triangle  $(\mathbf{l}_1, \mathbf{l}_2, \mathbf{l}_3)$  across one of the axes corresponds to remappings  $\varphi \rightarrow \pi - \varphi$  or  $\varphi \rightarrow -\varphi$  and hence a reversal in sign of the flat-sky bispectrum in Eq. (97). In this case the cancellation for flattened triangles discussed in Sec. VA does *not* apply. However since  $\sin 2\varphi_{31} \approx 2\varphi_{31} \ll 1$ , a suppression still exists.

The covariance of the  $B\Theta\Theta$  bispectrum is

$$\text{Cov} = C_{l_1}^{BB} C_{l_2}^{\Theta\Theta} C_{l_3}^{\Theta\Theta} \delta_{l_1 l'_1} \delta_{l_2 l'_2} \delta_{l_3 l'_3} + (l'_2 \leftrightarrow l'_3), \quad (99)$$

leading to a signal-to-noise

In a cosmic variance limited experiment (see Fig. 4), the  $B\Theta\Theta$  bispectrum has signal-to-noise advantages over its temperature and  $E$  polarization counterparts due to the fact that for scalar perturbations  $C_{l_1}^{BB}$  is dominated by the lensing contributions themselves. Moreover, even if the tensor contributions are near their current limits of  $T/S \leq 0.3$ , the signal-to-noise is not much affected for  $l \geq 100$  due to the strong damping of gravity wave contributions under the horizon scale at last scattering. However, for the Planck experiment, the detection is severely limited by detector noise and may also suffer further degradation from incomplete foreground subtraction [20].

Next, the  $BE\Theta$  bispectrum is given by

$$\begin{aligned} B_{l_1 l_2 l_3}^{BE\Theta} = & i({}_2F_{l_1 l_2 l_3} C_{l_2}^{E\phi} C_{l_3}^{\Theta E} + {}_2F_{l_1 l_3 l_2} C_{l_2}^{EE} C_{l_3}^{\Theta\phi}), \\ B_{(l_1, l_2, l_3)}^{BE\Theta} = & -(\mathbf{l}_2 \cdot \mathbf{l}_3) (\sin 2\varphi_{31} C_{l_2}^{E\phi} C_{l_3}^{\Theta E} + \sin 2\varphi_{21} C_{l_2}^{EE} C_{l_3}^{\Theta\phi}), \end{aligned} \quad (101)$$

with a covariance

$$\begin{aligned} \text{Cov} = & C_{l_1}^{BB} C_{l_2}^{EE} C_{l_3}^{\Theta\Theta} \delta_{l_1 l'_1} \delta_{l_2 l'_2} \delta_{l_3 l'_3} \\ & + C_{l_1}^{BB} C_{l_2}^{\Theta E} C_{l_3}^{\Theta E} \delta_{l_1 l'_1} \delta_{l_2 l'_2} \delta_{l_3 l'_2}, \end{aligned} \quad (102)$$

leading to a signal-to-noise

$$\left(\frac{S}{N}\right)^2 \geq \sum_{l_1 l_2 l_3} \frac{(B_{l_1 l_2 l_3}^{BE\Theta})^2}{2 C_{l_1}^{BB} C_{l_2}^{EE} C_{l_3}^{\Theta\Theta}}. \quad (103)$$

The signal-to-noise of this term can be greater than that of  $B\Theta\Theta$  due to the fact that the temperature and  $E$  polarization are only partially correlated in the unlensed sky.

Finally,

$$B_{l_1 l_2 l_3}^{BEE} = i({}_2F_{l_1 l_2 l_3} C_{l_2}^{E\phi} C_{l_3}^{EE} + (l_2 \leftrightarrow l_3)), \quad (104)$$

$$B_{(l_1, l_2, l_3)}^{BEE} = -(\mathbf{l}_2 \cdot \mathbf{l}_3) \sin 2\varphi_{31} C_{l_2}^{E\phi} C_{l_3}^{EE} - (\mathbf{l}_2 \leftrightarrow \mathbf{l}_3),$$

with a covariance

$$\text{Cov} = C_{l_1}^{BB} C_{l_2}^{EE} C_{l_3}^{EE} \delta_{l_1 l'_1} \delta_{l_2 l'_2} \delta_{l_3 l'_3} + (l'_2 \leftrightarrow l'_3), \quad (105)$$

leading to a signal-to-noise

$$\left(\frac{S}{N}\right)^2 = \sum_{l_1 l_2 l_3} \frac{(B_{l_1 l_2 l_3}^{BEE})^2}{2 C_{l_1}^{BB} C_{l_2}^{EE} C_{l_3}^{EE}}. \quad (106)$$

This signal vanishes for the ISW effect. Terms involving more than one  $B$  term have no contributions to first order in the correlation power spectrum.

## VI. DISCUSSION

We have shown that a harmonic approach to weak lensing in the CMB provides a simple and exact means of calculating its effects on the temperature and polarization power spectra, given the power spectrum of the lensing potential or convergence, and on the analogous bispectra given their power spectrum of the cross correlation with secondary anisotropies. Corrections to the flat-sky approximations appear even at high multipoles because even there, lensing effects arises from the large-scale fluctuations in the deflection angles. These corrections correspond to a change in the predictions at the  $\mu\text{K}$  level. While this is a negligible change given observations today, it is above the cosmic-variance limit and should be included when interpreting the high-precision results expected from Planck.

Unlike the temperature bispectrum, bispectra involving both the temperature and polarization multipoles of the CMB have the potential of producing a high signal-to-noise ( $\sim 10$ ) detection of secondary anisotropies such as the ISW effects even with relatively modest angular resolutions  $l < 1000$ . Other secondary anisotropies such as the Sunyaev-Zel'dovich effect are expected to contribute even stronger signals, although their exact amplitude is far more uncertain presently [4].

Achieving a cosmic-variance limited detection of the magnetic-parity polarization is a daunting challenge. Even signal-to-noise near unity requires detectors which are a factor of 3 more sensitive to polarization than those planned for the Planck satellite. Also of concern are the residual foreground contamination remaining in the maps after multifrequency subtraction. Our current best models of the foregrounds indicate that with the Planck channels and sensitivities, foregrounds and detector noise may enter into the polarization maps with comparable amplitudes [20]. Thus improving the actual sensitivity to the cosmic signal beyond the specifications of the Planck experiment will not only require better detectors but also a better understanding of the foregrounds, perhaps with increased frequency coverage and sampling. Nonetheless, the polarization of the CMB offers the potential to open a new window on physical processes at low redshifts and the opportunity to learn more from the CMB than can be achieved with the next generation of CMB satellites.

## ACKNOWLEDGMENTS

I would like to thank M. Zaldarriaga for many useful discussions and help during the early stages of this work. This work was supported by the Keck Foundation, the Sloan Foundation, and NSF-9513835.

## APPENDIX A: ALL-SKY WEAK LENSING OBSERVABLES

All weak lensing observables may be defined in terms of the projected potential  $\phi$

$$\phi(\hat{\mathbf{n}}) = -2 \int dD g_\phi(D) \Phi[\mathbf{x}(\hat{\mathbf{n}}), D], \quad (\text{A1})$$

or equivalently its multipole moments  $\phi_{lm}$  in the all-sky formalism or Fourier coefficients  $\phi(\mathbf{l})$ . Recall from Eq. (22) that  $g_\phi$  is the lensing efficiency function.

The deflection angle that a photon suffers while traveling from the source at  $D_s$  is given by the angular gradient of the potential  $\alpha(\hat{\mathbf{n}}) = \nabla \phi(\hat{\mathbf{n}})$ . Applying Eq. (56) to the spherical harmonic expansion, we obtain

$$\alpha = \sum_{lm} \sqrt{\frac{l(l+1)}{2}} \phi_{lm} [{}_1Y_l^m \mathbf{m}_+ - {}_{-1}Y_l^m \mathbf{m}_-]. \quad (\text{A2})$$

This implies that the quantity  $\alpha_1 \pm i\alpha_2$  is a spin  $\pm 1$  object

$$\begin{aligned} [\alpha_1 \pm i\alpha_2](\hat{\mathbf{n}}) &\equiv \sum_{lm} (c \pm ig)_{lm\pm 1} Y_l^m(\hat{\mathbf{n}}) \\ &= \pm \sum_{lm} \sqrt{l(l+1)} \phi_{lm\pm 1} Y_l^m(\hat{\mathbf{n}}), \end{aligned} \quad (\text{A3})$$

which states that the curl term  $c_{lm}$  vanishes and the gradient term

$$g_{lm} = -i\sqrt{l(l+1)} \phi_{lm}. \quad (\text{A4})$$

The power spectrum of the angular deflection is then

$$\langle g_{l'm'}^* g_{lm} \rangle \equiv \delta_{l,l'} \delta_{m,m'} C_l^{gg} = \delta_{l,l'} \delta_{m,m'} l(l+1) C_l^{\phi\phi}, \quad (\text{A5})$$

with the curl power vanishing. This accounts for the factors of  $l(l+1)$  in equations involving the angular deflection [e.g., Eq. (63)].

The corresponding flat-sky quantity is given by the decomposition [see Eq. (C8)]

$$[\alpha_1 \pm i\alpha_2](\hat{\mathbf{n}}) \equiv \pm i \int \frac{d^2l}{(2\pi)^2} [c \pm ig](\mathbf{l}) e^{\pm i(\varphi_l - \varphi)} e^{i\mathbf{l} \cdot \hat{\mathbf{n}}}, \quad (\text{A6})$$

with  $c(\mathbf{l}) = 0$  and

$$\begin{aligned} g(\mathbf{l}) &= -il\phi(\mathbf{l}), \\ C_{(l)}^{gg} &= l^2 C_{(l)}^{\phi\phi}. \end{aligned} \quad (\text{A7})$$

These relations also give the bispectrum of the deflection angle in terms of bispectrum of the lensing potential in the obvious manner.

The convergence ( $\kappa$ ) and shear ( $\gamma_1, \gamma_2$ ) are familiar weak lensing observables from galaxy weak lensing studies [15]. Although they are not directly needed for CMB studies, they are of interest for cross-correlation of galaxy weak-lensing maps and the CMB. An equivalent all-sky lensing treatment is given by Ref. [21].

These quantities are given by the second derivatives

$$\begin{aligned} \nabla_i \nabla_j \phi &\equiv \kappa g_{ij} + (\gamma_1 + i\gamma_2)(\mathbf{m}_+ \otimes \mathbf{m}_+)_{ij} \\ &\quad + (\gamma_1 - i\gamma_2)(\mathbf{m}_- \otimes \mathbf{m}_-)_{ij}, \end{aligned} \quad (\text{A8})$$

convergence where  $g_{ij}$  is the metric on the sphere. For the all-sky harmonics, it is useful to note that Eq. (55) implies

$$\begin{aligned} \nabla_i \nabla_j Y_l^m = & -\frac{l(l+1)}{2} Y_l^m g_{ij} + \frac{1}{2} \sqrt{\frac{(l+2)!}{(l-2)!}} [{}_2 Y_l^m(\mathbf{m}_+ \otimes \mathbf{m}_+) \\ & + {}_2 Y_l^m(\mathbf{m}_- \otimes \mathbf{m}_-)]_{ij}, \end{aligned} \quad (\text{A9})$$

and hence

$$\begin{aligned} \kappa(\hat{\mathbf{n}}) = & -\sum_{lm} \frac{1}{2} l(l+1) \phi_{lm} Y_l^m(\hat{\mathbf{n}}), \\ \gamma_1(\hat{\mathbf{n}}) \pm i \gamma_2(\hat{\mathbf{n}}) = & \sum_{lm} \frac{1}{2} \sqrt{\frac{(l+2)!}{(l-2)!}} \phi_{lm \pm 2} Y_l^m(\hat{\mathbf{n}}). \end{aligned} \quad (\text{A10})$$

Consequently, the power spectra are related as

$$\begin{aligned} C_l^{\kappa\kappa} = & \frac{l^2(l+1)^2}{4} C_l^{\phi\phi}, \\ C_l^{\epsilon\epsilon} = & \frac{1}{4} \frac{(l+2)!}{(l-2)!} C_l^{\phi\phi}, \\ C_l^{X\kappa} = & -\frac{1}{2} l(l+1) C_l^{X\phi}, \\ C_l^{X\epsilon} = & \frac{1}{2} \sqrt{\frac{(l+2)!}{(l-2)!}} C_l^{X\phi}, \end{aligned} \quad (\text{A11})$$

where the  $\epsilon$  shear power spectra is defined in the same way as that of the  $E$  polarization and  $X = \Theta, E, B$ . The  $\beta$  shear power is the analogue of the  $B$  polarization power and vanishes for weak lensing.

In the flat-sky limit, these expressions become

$$\begin{aligned} \kappa(\hat{\mathbf{n}}) = & -\frac{1}{2} \int \frac{d^2 \mathbf{l}}{(2\pi)^2} l^2 \phi(\mathbf{l}) e^{i\mathbf{l} \cdot \hat{\mathbf{n}}}, \\ \gamma_1(\hat{\mathbf{n}}) \pm i \gamma_2(\hat{\mathbf{n}}) = & -\frac{1}{2} \int \frac{d^2 \mathbf{l}}{(2\pi)^2} l^2 \phi(\mathbf{l}) e^{\pm 2i(\varphi_l - \varphi)} e^{i\mathbf{l} \cdot \hat{\mathbf{n}}}, \end{aligned} \quad (\text{A12})$$

so that

$$\begin{aligned} C_{(l)}^{\kappa\kappa} = C_{(l)}^{\epsilon\epsilon} = & \frac{1}{4} l^4 C_{(l)}^{\phi\phi}, \\ C_{(l)}^{X\kappa} = -C_{(l)}^{X\epsilon} = & -\frac{1}{2} l^2 C_{(l)}^{X\phi}. \end{aligned} \quad (\text{A13})$$

These relations also give the bispectrum of the shear and convergence in terms of the bispectrum of the lensing potential

$$B_{l_1 l_2 l_3}^{\kappa\kappa\kappa} = \frac{1}{8} [l_1(l_1+1)l_2(l_2+1)l_3(l_3+1)] B_{l_1 l_2 l_3}^{\phi\phi\phi},$$

$$B_{l_1 l_2 l_3}^{\epsilon\epsilon\epsilon} = \frac{1}{8} \sqrt{\frac{(l_1+2)! (l_2+2)! (l_3+2)!}{(l_1-2)! (l_2-2)! (l_3-2)!}} B_{l_1 l_2 l_3}^{\phi\phi\phi}, \quad (\text{A14})$$

with a similar relation for the flat-sky bispectra.

## APPENDIX B: WIGNER-3j EVALUATION

### 1. Exact expressions

The expressions for the power spectrum of the lensed temperature and polarization distributions involve specific sets of Wigner-3j symbols that can be efficiently evaluated. The expression for the temperature involves a set which has a closed algebraic form

$$\begin{aligned} \begin{pmatrix} l_1 & l_2 & l_3 \\ 0 & 0 & 0 \end{pmatrix} = & (-1)^{L/2} \frac{(L/2)!}{(L/2-l_1)! (L/2-l_2)! (L/2-l_3)!} \\ & \times \left[ \frac{(L-2l_1)! (L-2l_2)! (L-2l_3)!}{(L+1)!} \right]^{1/2}, \end{aligned} \quad (\text{B1})$$

for even  $L = l_1 + l_2 + l_3$  and zero for odd  $L$ .

The required set for the polarization does not have an exact closed form expression. However it may be equally efficiently evaluated for our purposes with the realization that in the sums, we require

$$\begin{pmatrix} l_1 & l_2 & l_3 \\ m_1 & m_2 & m_3 \end{pmatrix} \equiv w_{l_1} \quad (\text{B2})$$

for fixed  $l_2, l_3, m_1, m_2, m_3$  and all allowed  $l_1$ . The recursion relations for the Wigner-3j symbol

$$l_1 A_{l_1+1} w_{l_1+1} + B_{l_1} w_{l_1} + (l_1+1) A_{l_1} w_{l_1-1} = 0, \quad (\text{B3})$$

where

$$\begin{aligned} A_{l_1} = & \sqrt{l_1^2 - (l_2 - l_3)^2} \sqrt{(l_2 + l_3 + 1)^2 - l_1^2} \sqrt{l_1^2 - m_1^2}, \\ B_{l_1} = & -(2l_1 + 1) [l_2(l_2 + 1)m_1 - l_3(l_3 + 1)m_1 \\ & - l_1(l_1 + 1)(m_3 - m_2)], \end{aligned} \quad (\text{B4})$$

allow us to generate the whole set at once [22]. For a stable recursion, one begins at the minimum and maximum  $l_1$  values

$$\begin{aligned} l_{1\min} = & \max(|l_2 - l_3|, |m_1|), \\ l_{1\max} = & l_2 + l_3, \end{aligned} \quad (\text{B5})$$

with  $w_{l_{1\min}} = w_{l_{1\max}} = 1$  and carries the recursion in both directions to the midpoint  $l_{1\text{mid}}$  in the range (or any non-vanishing entry in the vicinity). One then renormalizes either the left or right recursion to make the  $w_{l_{1\text{mid}}}$  agree. The remaining overall normalization is fixed by requiring

$$\sum_{l_1} (2l_1 + 1)w_{l_1}^2 = 1 \quad (\text{B6})$$

and

$$\text{sgn}(w_{l_{1\max}}) = (-1)^{l_2 - l_3 - m_1}. \quad (\text{B7})$$

Putting these relations together, we obtain the full set of symbols as required.

## 2. Approximations

We can use the general relation between the all and flat sky bispectra of Eq. (20) compared with the explicit calculation of the flat sky bispectrum in Sec. VB to develop an high- $l$  approximation for the specific symbol in the polarization calculations. The comparison implies that

$$\begin{pmatrix} l_1 & l_2 & l_3 \\ 2 & 0 & -2 \end{pmatrix} \approx \cos 2\varphi_{31} \begin{pmatrix} l_1 & l_2 & l_3 \\ 0 & 0 & 0 \end{pmatrix}, \quad (\text{B8})$$

for  $L = l_1 + l_2 + l_3 = \text{even}$ . By the law of cosines,

$$\cos 2\varphi_{31} = \frac{1}{2} \frac{(l_2^2 - l_1^2 - l_3^2)^2}{l_1^2 l_3^2} - 1. \quad (\text{B9})$$

Then

$$\begin{aligned} \begin{pmatrix} l_1 & l_2 & l_3 \\ 2 & 0 & -2 \end{pmatrix} &\approx (-1)^{L/2} \left[ \frac{1}{2} \frac{(l_2^2 - l_1^2 - l_3^2)^2}{l_1^2 l_3^2} - 1 \right] \\ &\times \frac{(L/2)!}{(L/2 - l_1)! (L/2 - l_2)! (L/2 - l_3)!} \\ &\times \left[ \frac{(L - 2l_1)! (L - 2l_2)! (L - 2l_3)!}{(L + 1)!} \right]^{1/2}, \end{aligned}$$

for  $L = \text{even}$ . For odd values of  $L$ , we use the relation

$$\begin{pmatrix} l_1 & l_2 & l_3 \\ 2 & 0 & -2 \end{pmatrix} \approx \pm i \sin 2\varphi_{31} \begin{pmatrix} l_1 & l_2 & l_3 \\ 0 & 0 & 0 \end{pmatrix}, \quad (\text{B10})$$

and fix the overall sign ambiguity by an explicit evaluation. By the triangle relations

$$\begin{aligned} \sin 2\varphi_{31} &= \mp \frac{1}{2} [L(L - 2l_1)(L - 2l_2)(L - 2l_3)]^{1/2} \\ &\times \left( \frac{l_2^2 - l_1^2 - l_3^2}{l_1^2 l_3^2} \right). \end{aligned}$$

Putting this together with Eq. (B1) and fixing the sign ambiguity, we obtain

$$\begin{aligned} \begin{pmatrix} l_1 & l_2 & l_3 \\ 2 & 0 & -2 \end{pmatrix} &\approx (-1)^{(L-1)/2} \frac{1}{2} \left( \frac{l_2^2 - l_1^2 - l_3^2}{l_1^2 l_3^2} \right) \\ &\times \frac{(L/2)!}{(L/2 - l_1)! (L/2 - l_2)! (L/2 - l_3)!} \end{aligned}$$

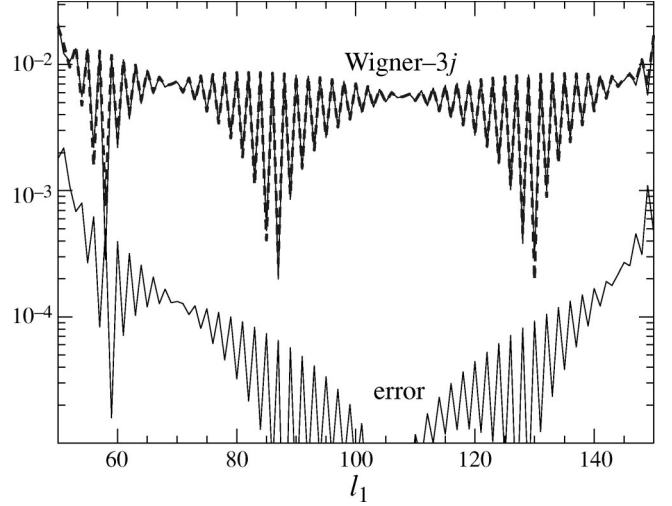


FIG. 5. Wigner-3j function and approximation. An example of the Wigner-3j symbol relevant to the polarization calculation with  $l_2 = 100$ ,  $m_2 = 0$ ,  $l_3 = 50$ ,  $m_3 = -2$  is shown as calculated from the recursion relations (solid upper) and analytic approximation (dashed). The difference is shown below (solid lower).

$$\begin{aligned} &\times \left[ \frac{L(L - 2l_1)(L - 2l_2)(L - 2l_3)}{(L + 1)!} \right]^{1/2} \\ &\times \frac{(L - 2l_1)! (L - 2l_2)! (L - 2l_3)!}{(L + 1)!} \end{aligned} \quad (\text{B11})$$

for  $L = \text{odd}$ . The half integer factorials are defined by the gamma function  $x! = \Gamma(1 + x)$ . By explicit calculation we find that these expressions are valid to better than 3% of the rms amplitude of the symbol when averaged over neighboring  $l$  for all  $l_1 - |l_2 - l_3| \geq 25$  and  $l_2 + l_3 - l_1 \geq 25$ , i.e., for triangles that are sufficiently far from being flat. Near zero crossings, the *fractional* error can be large but the absolute error remains a small fraction of the rms. A typical case is shown in Fig. 5.

These relations may be useful in cases where only a single symbol is needed. However, for the lensing calculation where the whole set is required, the recursion relations are as efficient as the approximation and are exact.

## APPENDIX C: FLAT AND ALL SKY CORRESPONDENCE

### 1. Harmonics

We establish here the correspondence between the all and flat sky harmonic coefficients of spin zero (scalar), spin one (vector), and spin two (tensor) quantities on the sky. Following Ref. [23], let us begin by introducing the following weighted sum over the multipole moments of the field  $X = \Theta$ ,  $E$ ,  $B$ , or  $\phi$  for a given  $l$  and its inverse relation:

$$\begin{aligned} X(\mathbf{l}) &= \sqrt{\frac{4\pi}{2l+1}} \sum_m i^{-m} X_{lm} e^{im\varphi_l}, \\ X_{lm} &= \sqrt{\frac{2l+1}{4\pi}} i^m \int \frac{d\varphi_l}{2\pi} e^{-im\varphi_l} X(\mathbf{l}). \end{aligned} \quad (\text{C1})$$

The goal is then to show that this quantity is the Fourier coefficient of the flat-sky expansion.

Spin-0 quantities, such as the temperature fluctuations and the lensing potential, are decomposed as

$$X(\hat{\mathbf{n}}) = \sum_{lm} X_{lm} Y_l^m(\hat{\mathbf{n}}). \quad (\text{C2})$$

For small angles around the pole, the spherical harmonics may be approximated as<sup>1</sup>

$$Y_l^m \approx J_m(l\theta) \sqrt{\frac{l}{2\pi}} e^{im\varphi}, \quad (\text{C3})$$

and the expansion of the plane wave

$$e^{i\mathbf{l}\cdot\hat{\mathbf{n}}} = \sum_m i^m J_m(l\theta) e^{im(\varphi-\varphi_l)} \approx \sqrt{\frac{2\pi}{l}} \sum_m i^m Y_l^m e^{im\varphi_l}. \quad (\text{C4})$$

Thus

$$\begin{aligned} X(\hat{\mathbf{n}}) &= \sum_{lm} X_{lm} Y_l^m \\ &\approx \sum_l \frac{l}{2\pi} \int \frac{d\varphi_l}{2\pi} X(\mathbf{l}) \sum_m J_m(l\theta) i^m e^{im(\varphi-\varphi_l)} \\ &\approx \int \frac{d^2l}{(2\pi)^2} X(\mathbf{l}) e^{i\mathbf{l}\cdot\hat{\mathbf{n}}}, \end{aligned} \quad (\text{C5})$$

which is the desired correspondence.

Spin-1 quantities such as the deflection angles are decomposed as

$$\pm X(\hat{\mathbf{n}}) = \sum_{lm} \pm X_{lm\pm 1} Y_l^m. \quad (\text{C6})$$

Here one notes that

$$\pm_1 Y_l^m \approx \pm \frac{1}{l} e^{\mp i\varphi} (\partial_x \pm i\partial_y) Y_l^m, \quad (\text{C7})$$

and thus

$$\begin{aligned} \pm X(\hat{\mathbf{n}}) &= \sum_{lm} \pm X_{lm\pm 1} Y_l^m \\ &\approx \pm \sum_l \frac{l}{2\pi} \int \frac{d\varphi_l}{2\pi} \pm X(\mathbf{l}) e^{\mp i\varphi} \frac{1}{l} (\partial_x \pm i\partial_y) e^{i\mathbf{l}\cdot\hat{\mathbf{n}}} \\ &\approx \pm i \int \frac{d^2l}{(2\pi)^2} \pm X(\mathbf{l}) e^{\pm i(\varphi_l-\varphi)} e^{i\mathbf{l}\cdot\hat{\mathbf{n}}}. \end{aligned} \quad (\text{C8})$$

Finally, spin-2 quantities such as the polarization are decomposed as

$$\pm X(\hat{\mathbf{n}}) = \sum_{lm} \pm X_{lm\pm 2} Y_l^m. \quad (\text{C9})$$

Here one notes that

$$\pm_2 Y_l^m \approx \frac{1}{l^2} e^{\mp 2i\varphi} (\partial_x \pm i\partial_y)^2 Y_l^m, \quad (\text{C10})$$

and thus

$$\begin{aligned} \pm X(\hat{\mathbf{n}}) &= \sum_{lm} \pm X_{lm\pm 2} Y_l^m \\ &\approx \sum_l \frac{l}{2\pi} \int \frac{d\varphi_l}{2\pi} \pm X(\mathbf{l}) e^{\mp 2i\varphi} \frac{1}{l^2} (\partial_x \pm i\partial_y)^2 e^{i\mathbf{l}\cdot\hat{\mathbf{n}}} \\ &\approx - \int \frac{d^2l}{(2\pi)^2} \pm X(\mathbf{l}) e^{\pm 2i(\varphi_l-\varphi)} e^{i\mathbf{l}\cdot\hat{\mathbf{n}}}, \end{aligned} \quad (\text{C11})$$

as desired.

## 2. Power spectra

The correspondence between power spectra then follows from the relationship between the harmonics

$$\begin{aligned} \langle X_{lm}^* X_{l'm'} \rangle &\approx i^{m'-m} \frac{\sqrt{ll'}}{2\pi} C_{(l)}^{XX'} \int d\varphi_l e^{im\varphi_l} \\ &\quad \times \int d\varphi_{l'} e^{-im'\varphi_{l'}} \delta(\mathbf{l}-\mathbf{l}'). \end{aligned} \quad (\text{C12})$$

We then expand the delta function in plane waves

$$\begin{aligned} \delta(\mathbf{l}-\mathbf{l}') &= \int \frac{d\hat{\mathbf{n}}}{(2\pi)^2} e^{i(\mathbf{l}-\mathbf{l}')\cdot\hat{\mathbf{n}}} \\ &\approx \frac{2\pi}{\sqrt{ll'}} \int \frac{d\hat{\mathbf{n}}}{(2\pi)^2} \sum_{mm'} i^{m-m'} Y_{l'}^{m'} * Y_l^m e^{im\varphi_l - im'\varphi_{l'}}. \end{aligned} \quad (\text{C13})$$

Integrating over the azimuthal angles  $\varphi_l, \varphi_{l'}$  collapses the sum to

$$\begin{aligned} \langle X_{lm}^* X_{l'm'} \rangle &\equiv \delta_{l,l'} \delta_{m,m'} C_l^{XX'} \\ &\approx C_{(l)}^{XX'} \int d\hat{\mathbf{n}} Y_l^{-m} * Y_{l'}^{-m'} \\ &= \delta_{l,l'} \delta_{m,m'} C_{(l)}^{XX'} \end{aligned} \quad (\text{C14})$$

which proves the desired relation in Eq. (20)

$$C_l^{XX'} \approx C_{(l)}^{XX'}. \quad (\text{C15})$$

<sup>1</sup>Note that our definition of  $Y_l^m$  differs from the usual one by  $(-1)^m$  to conform with the spin spherical harmonic convention [22].

### 3. Bispectra

The correspondence between bispectra is established in exactly the same way as with the power spectra. The only difference is that the expansion of  $\delta(\mathbf{l}' - \mathbf{l})$  in Eq. (C14) is replaced with that of  $\delta(\mathbf{l}_1 + \mathbf{l}_2 + \mathbf{l}_3)$  leading to

$$\begin{aligned} \langle X_{lm} X'_{l'm'} X''_{l''m''} \rangle &\equiv \begin{pmatrix} l & l' & l'' \\ m & m' & m'' \end{pmatrix} B_{ll'l''}^{XX'X''} \\ &\approx B_{(l,l',l'')}^{XX'X''} \int d\hat{\mathbf{n}} Y_l^{-m} Y_{l'}^{-m'} Y_{l''}^{-m''} \\ &= B_{(l,l',l'')}^{XX'X''} \begin{pmatrix} l & l' & l'' \\ 0 & 0 & 0 \end{pmatrix} \begin{pmatrix} l & l' & l'' \\ m & m' & m'' \end{pmatrix} \\ &\quad \times \sqrt{\frac{(2l+1)(2l'+1)(2l''+1)}{4\pi}}. \end{aligned} \quad (\text{C16})$$

This establishes the relation

$$\begin{aligned} B_{ll'l''}^{XX'X''} &\approx \begin{pmatrix} l & l' & l'' \\ 0 & 0 & 0 \end{pmatrix} \\ &\quad \times \sqrt{\frac{(2l+1)(2l'+1)(2l''+1)}{4\pi}} B_{(l,l',l'')}^{XX'X''}. \end{aligned} \quad (\text{C17})$$

Note that we have implicitly assumed that the bispectrum only depends on the the magnitudes  $(l, l', l'')$  so that it may be removed from the azimuthal integrals. This is not true for terms not involving the magnetic parity. In this case, the sign of the flat-sky bispectrum depends on orientation but we find empirically that a similar relationship holds up to a sign ambiguity as discussed in Sec. II B.

### 4. Signal-to-noise

Here we establish the correspondence between the all and flat sky signal-to-noise statistics for the case of diagonal contributions to the covariance matrix [ $\text{Cov} = \text{diag}(\text{Var})$ ],

$$\left(\frac{S}{N}\right)^2 = \sum_{lm} \frac{(C_l^{XX})^2}{\text{Var}} = \sum_l (2l+1) \frac{(C_l^{XX})^2}{\text{Var}}. \quad (\text{C18})$$

For the flat sky case, one defines a weighted sum of Fourier harmonics

$$P = \int d^2l W(l) X(\mathbf{l}) X(-\mathbf{l}), \quad (\text{C19})$$

with optimal weights given by  $W(l) = C_{(l)}^{XX}/\text{Var}$  from which one calculates the signal-to-noise  $\langle P \rangle^2 / \langle P^2 \rangle$  as

$$\left(\frac{S}{N}\right)^2 = \frac{f_{\text{sky}}}{\pi} \int d^2l \frac{[C_{(l)}^{XX}]^2}{\text{Var}} \approx 2f_{\text{sky}} \int l dl \frac{(C_l^{XX})^2}{\text{Var}}, \quad (\text{C20})$$

where we have used the fact that  $\delta(\mathbf{0}) \approx V/(2\pi^2) = f_{\text{sky}}/\pi$ . These expressions agree in the high  $l$  limit and imply the familiar result that  $f_{\text{sky}}$  should multiply the signal-to-noise of angular power spectrum measurements given incomplete sky coverage.

The bispectrum signal-to-noise similarly is

$$\begin{aligned} \left(\frac{S}{N}\right)^2 &= \sum_{l_1 l_2 l_3} \frac{(B_{l_1 l_2 l_3}^{XXX})^2}{\text{Var}} \sum_{m_1 m_2 m_3} \begin{pmatrix} l_1 & l_2 & l_3 \\ m_1 & m_2 & m_3 \end{pmatrix}^2 \\ &= \sum_{l_1 l_2 l_3} \frac{(B_{l_1 l_2 l_3}^{XXX})^2}{\text{Var}}, \end{aligned} \quad (\text{C21})$$

for the all sky bispectrum and

$$\left(\frac{S}{N}\right)^2 = \frac{f_{\text{sky}}}{\pi} \frac{1}{(2\pi)^2} \int d^2l_1 \int d^2l_2 \frac{[B_{(l_1, l_2, l_3)}^{XXX}]^2}{\text{Var}}, \quad (\text{C22})$$

for the flat sky bispectrum [5]. The extra factor of  $(2\pi)^2$  compared with the power spectrum is from the extra delta function in the noise term. One can show that these expressions agree in the high- $l$  limit by restoring the integration over  $l_3$ , expanding the delta function into spherical harmonics as in Eq. (C13), and integrating over azimuthal angles

$$\begin{aligned} &\int d^2l_1 \int d^2l_2 \int d^2l_3 \delta(\mathbf{l}_1 + \mathbf{l}_2 + \mathbf{l}_3) \\ &\approx \int l_1 dl_1 \int l_2 dl_2 \int l_3 dl_3 \sqrt{\frac{(2\pi)^5}{l_1 l_2 l_3}} \int d\hat{\mathbf{n}} Y_{l_1}^0 Y_{l_2}^0 Y_{l_3}^0 \\ &\approx 8\pi^2 \int l_1 dl_1 \int l_2 dl_2 \int l_3 dl_3 \begin{pmatrix} l_1 & l_2 & l_3 \\ 0 & 0 & 0 \end{pmatrix}^2. \end{aligned} \quad (\text{C23})$$

With the general correspondence of bispectra from Eq. (C17), this becomes

$$\left(\frac{S}{N}\right)^2 \approx f_{\text{sky}} \int dl_1 \int dl_2 \int dl_3 \frac{(B_{l_1 l_2 l_3}^{XXX})^2}{\text{Var}}, \quad (\text{C24})$$

which proves the equivalence of the signal-to-noise for high  $l$  and  $f_{\text{sky}} = 1$ .

[1] A. Blanchard and J. Schneider, *Astron. Astrophys.* **184**, 1 (1987); A. Kashlinsky, *Astrophys. J. Lett.* **331**, L1 (1988); E. V. Linder, *Astron. Astrophys.* **206**, 199 (1988); S. Cole and G. Efstathiou, *Mon. Not. R. Astron. Soc.* **239**, 195 (1989); M. Sasaki, *ibid.* **240**, 415 (1989); K. Watanabe and K. Tomita,

*Astrophys. J.* **370**, 481 (1991); M. Fukugita, T. Futamase, M. Kasai, and E. L. Turner, *ibid.* **393**, 3 (1992); L. Cayon, E. Martinez-Gonzalez, and J. L. Sanz, *Astrophys. J.* **413**, 10 (1993).

[2] U. Seljak, *Astrophys. J.* **463**, 1 (1996).

- [3] M. Zaldarriaga and U. Seljak, Phys. Rev. D **58**, 023003 (1998).
- [4] D. M. Goldberg and D. N. Spergel, Phys. Rev. D **59**, 103002 (1999).
- [5] M. Zaldarriaga, astro-ph/9910498.
- [6] U. Seljak and M. Zaldarriaga, Astrophys. J. **469**, 437 (1996).
- [7] D. J. Eisenstein and W. Hu, Astrophys. J. **511**, 5 (1999).
- [8] E. F. Bunn and M. White, Astrophys. J. **480**, 6 (1997).
- [9] P. J. E. Peebles, *The Large-Scale Structure of the Universe* (Princeton University Press, Princeton, 1980).
- [10] U. Seljak and M. Zaldarriaga, Phys. Rev. D **60**, 043504 (1999).
- [11] J. N. Goldberg *et al.*, J. Math. Phys. **7**, 863 (1967).
- [12] M. Kamionkowski, A. Kosowsky, and A. Stebbins, Phys. Rev. D **55**, 7368 (1997).
- [13] M. Zaldarriaga and U. Seljak, Phys. Rev. D **55**, 1830 (1997).
- [14] N. Kaiser, Astrophys. J. **498**, 26 (1998).
- [15] M. Bartelmann and P. Schneider, astro-ph/9912508.
- [16] J. A. Peacock and S. J. Dodds, Mon. Not. R. Astron. Soc. **280**, L19 (1996).
- [17] W. Hu and M. White, Phys. Rev. D **56**, 596 (1997).
- [18] X. Luo, Astrophys. J. **427**, 71 (1994).
- [19] A. Cooray and W. Hu, astro-ph/9910397.
- [20] M. Tegmark, D. J. Eisenstein, W. Hu, and A. de Oliveira-Costa, Astrophys. J. **530**, 133 (2000).
- [21] A. Stebbins, astro-ph/9609149.
- [22] K. Schulten and R. G. Gordon, J. Math. Phys. **16**, 1971 (1975).
- [23] M. White, J. E. Carlstrom, M. Dragovan, and W. L. Holzapfel, Astrophys. J. **514**, 12 (1999).